IUCN WATER AND NATURE INITIATIVE

PANGANI BASIN WATER BOARD[1]

PANGANI RIVER BASIN FLOW ASSESSMENT

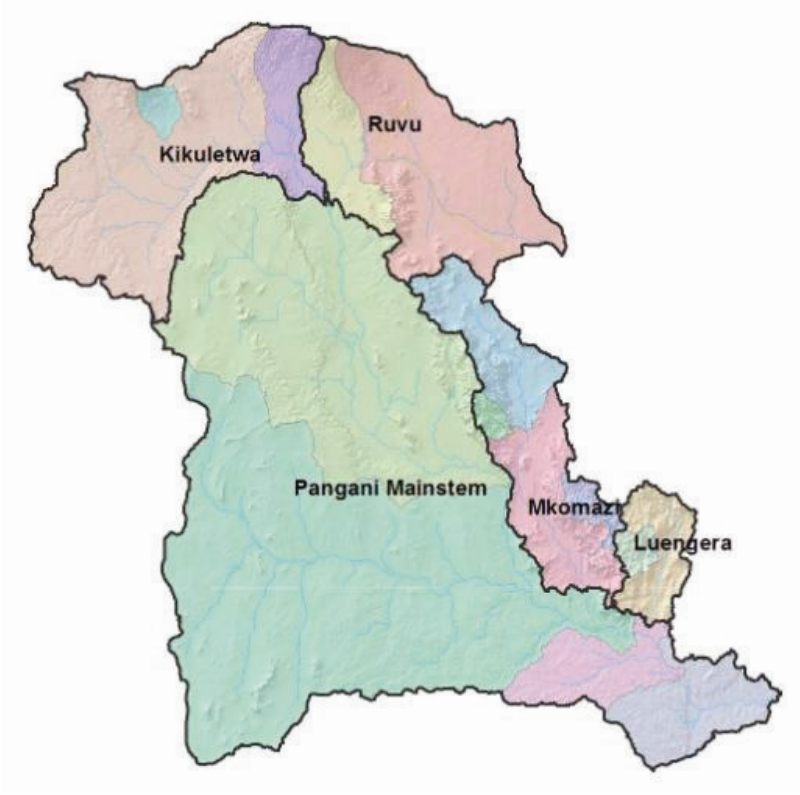

Development of Climate change Scenarios

S.H. Mkhandi, P. Valimba and T.A. Kimaro

June 2008

[1] As of 2010, Pangani Basin Water Office is known as Pangani Basin Water Board

Published by: Pangani Basin Water Board (PBWB)
International Union for Conservation of Nature (IUCN)

Citation: PWBO/IUCN. 2008. Development of Climate change scenarios. Pangani River Basin Flow Assessment. Pangani Basin Water Board, Moshi and IUCN Eastern and Southern Africa Regional Programme. Vii+53 pp.

Available from: IUCN - ESARO Publications Service Unit, P. O. Box 68200 - 00200, Nairobi, Kenya;
Telephone ++ 254 20 890605-12; Fax ++ 254 20 890615; E-mail: earo@iucn.org

Addendum 1

The climate change modeling in this report was undertaken by experts from the University of Dar es Salaam. Its purpose was to model and come up with information that could predict what would happen to flows in the Pangani Basin in the future.

After international review by UNDP and University of Cape Town climate specialists, the modelling was considered to have too many uncertainties in the results and temperatures were in low range compared to recent studies. The challenge has been getting reliable data, and the study providing the background to the scenario in this report showed that the Pangani area would get drier, whereas the latest International Panel on Climate Change (IPCC) report and the information from the international reviewers indicated that the area will get wetter.

Following from recommendations by the reviewers, the project steering committee made the decision to commission a detail climate change modeling study of the Pangani Basin through the Climate Change Analysis Group at the University of Cape Town.

The information in this report is the original climate change modeling and the results should not be considered as the likely climate future. However, there is useful information within the report on climate and data which can be used for reference purposes.

PANGANI BASIN MANAGEMENT PROJECT

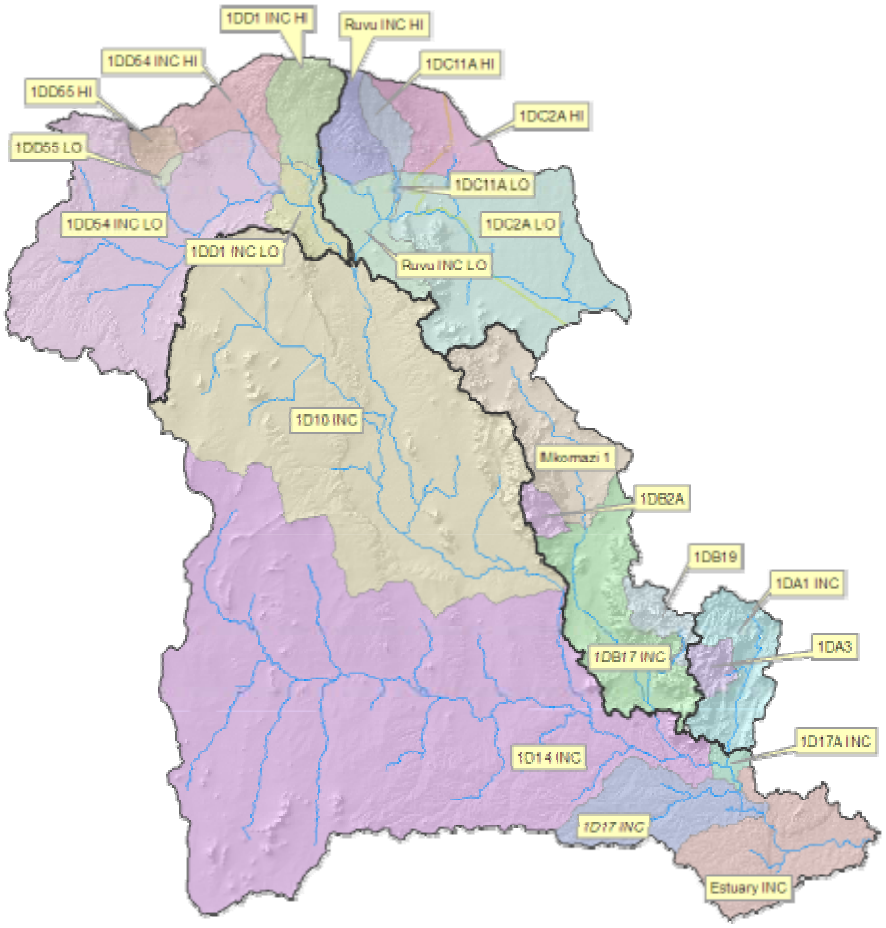

DEVELOPMENT OF CLIMATE CHANGE SCENARIOS

FINAL DRAFT

By

Dr Simon H MKHANDI

Dr Patrick VALIMBA

Dr Tumaini A KIMARO

June 2008

Executive Summary

The Terms of Reference for this study were to provide modified rainfall and evaporation series for each of the selected 16 catchments in the Pangani River Basin under scenarios of climate change. Statistical downscaling was used to establish multiple linear regression (MLR) models between observed monthly rainfall and NCEP/NCAR re-analyses for the period 1961-2001. Established models gave moderately good to better efficiencies for majority of catchments although rainfall in some months could not be better predicted. However, downscaled monthly rainfall using HadCM3 were poorly predicted and the use of GFDL CM2.1 improved significantly rainfall prediction with no predictions of negative rainfalls. The resulting downscaled rainfall indicated significant changes will be experienced during the months October to January leading to declining predominantly orographic rainfall in these months. An increase of rainfall is predicted during the long rains particularly in April and May and the dry season (June-September) particularly in June suggesting a protrusion of long rains into the dry season. Calibration of MLR models for evaporation could not be achieved due to lack of time series of evaporation and more time is required to establish the scarce available information from hardcopies. However, the highest ratio of 1.368 temperature predictions of between December-February (DJF) and June-August (JJA) and annual evaporation rise of 20% by the year 2100 were used to modify available average monthly evaporation to provide evaporation scenarios for 2020s, 2050s and 2080s.

Table of Contents

Executive Summary i
Table of Contents ii
List of Tables iv
List of Figure v
Acronyms vi
1 INTRODUCTION 1
1.1 BACKGROUND 1
1.2 OBJECTIVES 1
2 LITERATURE REVIEW 2
2.1 INTRODUCTION 2
2.2 FUTURE CLIMATE PREDICTIONS FOR PANGANI 2
2.2.1 General Circulation models (GCMs) 2
2.2.1.1 Types 2
2.2.1.2 Available CGCMs 2
2.2.1.3 Emission scenarios 3
2.2.1.3.1 IS92 emission scenarios 4
2.2.1.3.2 SRES emission scenarios 5
2.2.1.4 Selection and application of GCM climate change scenarios 7
2.2.1.4.1 Selection of GCM climate change scenarios 7
2.2.1.4.2 Application of GCM climate change scenarios 9
2.2.2 Downscaling of GCM outputs 9
2.2.2.1 Spatial downscaling 10
2.2.2.1.1 Statistical downscaling 11
2.2.2.1.2 Dynamical downscaling 12
2.2.2.2 Temporal downscaling 13
3 DATA AND METHODOLOGY 14
3.1 INTRODUCTION 14
3.2 DATA 14
3.2.1 Rainfall and climatic data 14
3.2.2 Re-analysis data 14
3.2.3 GCM output data 15
3.3 METHODOLOGY 16
3.3.1 Selection of downscaling method 16
3.3.2 Development of rainfall/evaporation prediction models 19
3.3.2.1 Selection of climatic predictors and influencing regions 19
3.3.2.2 Establishment of rainfall/evaporation prediction models 20
3.3.2.2.1 MLR model calibration 20
3.3.2.2.2 MLR model evaluation 21
3.3.3 Assessment of GCM capability 21
3.3.4 Development of future rainfall and evaporation series 21
4 FUTURE RAINFALL AND EVAPORATION SERIES FOR PANGANI 23
4.1 INTRODUCTION 23
4.2 RAINFALL AND EVAPORATION DOWNSCALING 23
4.2.1 Selection of climatic predictors for rainfall 23
4.2.2 Selection of climatic predictors for evaporation 24
4.2.3 Calibration and verification of rainfall models 27
4.2.4 GCM prediction capability 28
4.2.4.1 Selection of suitable GCMs 28
4.2.4.2 Assessment of efficiency of selected GCMs 28

4.3 MODIFIED RAINFALL AND EVAPORATION SERIES 31
4.3.1 Modified rainfall series 31
4.3.1.1 Rainfall series for average conditions 31
4.3.1.2 Correction for future rainfall scenarios 32
4.3.1.3 Discussion of developed future rainfall scenarios 35
4.3.1.4 Rainfall series for wet and dry conditions 37
4.3.2 Modified evaporation series 38
5 CONCLUSIONS 43
6 REFERENCES 44
APPENDICES 46

List of Tables

Table 2.1: Information of available coupled GCMs. 3
Table 2.2: Available coupled GCMs SRES scenario runs. 8
Table 3.1: Available coupled GCMs SRES A2 scenario runs outputs. 17
Table 4.2: Example of changing CE (%) for different periods in 1961-2001. 27
Table 4.3: Model efficiency criterion (CE) between observed catchment monthly rainfall in Pangani and observed climatic predictors for the 1980-2001 period. Moderate efficiencies are shown in blue. 28
Table 4.4: IVF between observed catchment monthly rainfall in Pangani and NCEP/NCAR, HADCM3 and GFDL CGCM2.1 estimated monthly rainfall for the 1980-2001 period. Negative IVF are in italics. 29
Table 4.5: IVF between observed catchment monthly rainfall in Pangani and NCEP/NCAR and GFDL CGCM2.1 estimated monthly rainfall for the 1980-2001 period for modified MLR model parameters. 31
Table 4.6: Simulated changes (%) of monthly rainfall in Pangani. Decreases are yellow filled, increases are light blue filled. 33
Table 4.7: Corrected simulated changes (%) of monthly rainfall in Pangani. Decreases are yellow filled, increases are light blue filled. 34
Table 4.8: Predicted changes (%) of seasonal rainfall in Pangani expressed from the 1980-1999 averages. Decreases are yellow filled, increases are light blue filled. 36
Table 4.9: Available average monthly evaporation (mm) in Pangani basin. 39
Table 4.10: Adjusted modification factors for monthly evaporation in Pangani basin for the 2020s. 40
Table 4.11: Modification factors for monthly evaporation in Pangani basin for the 2050s. 41
Table 4.12: Modification factors for monthly evaporation in Pangani basin for the 2080s. 41
Table 4.13: Present-day and 2080s projected changes (%) of monthly evaporation in Pangani: Highest – red, Lowest – blue. 42
Table 4.14: 2080s projected changes (mm) of monthly evaporation in Pangani. 42

List of Figure

Fig 2.1: Global-mean temperature change (°C) associated with the six IS92 emissions scenarios. 5
Fig 2.2: A schematic representation of the SRES scenario family. The A1 and A2 families have a more economic focus than B1 and B2, which are more environmental, whilst the focus of A1 and B1 is more global compared to the more regional A2 and B2. 6
Fig 2.3: Global-mean temperature change (°C) associated with the six SRES marker scenarios, A1FI, A1T, A1B, A2, B1 and B2. 7
Fig 2.4: A schematic illustration of general spatial downscaling process (Source: SDSM Manual). 10
Fig 2.5: The transfer approach to spatial downscaling (Source: http://www.ceaa-acee.gc.ca/015/001/004/PDF/Figure15_e.pdf)..... 11
Fig 3.1: Location of catchments established and made available for the study. 15
Fig 3.2: Location of gridboxes where oceanic and atmospheric variables have an influence on Pangani rainfall. 18
Fig 4.1: Sources of moisture for and moisture transporting winds into Pangani. 24
Fig 4.2: Location of atmospheric predictors: zonal winds (crosses) and 850hPa relative humidity (circles) in the Western Indian Ocean. 25
Fig 4.2: Comparison of NCEP/NCAR, HadCM3 and GFDL CM2.1 a) October and b) December zonal winds at gridboxes in Southwest Indian Ocean..... 30
Fig 4.3: Rainfall changes between 1961 and 2099 at a) 1da1 and b) 1d10. 35
Fig 4.4: Time series of observed November catchment rainfall at 1DC2A. 38
Fig 4.5: Time series of 2050 November rainfall amounts at 1DC2A for average, wetter and drier conditions. 38

Acronyms

AGCM	Atmospheric General Circulation Model
AOM	Atmosphere Ocean Model
CCCMa	Canadian Centre for Climate Modelling and Analysis
CCIS	Canadian Climate Impacts Scenarios
CCSR98	Centre for Climate Research Studies Model version 98
CE	Coefficient of Efficiency
CICS	Canadian Institute for Climate Studies
CGCM	Coupled General Circulation Model
CGCM1/2	Canadian General Circulation Model Versions 1 and 2
CLIGEN	Climate Generator
CNRM	Centre National de Recherche Météorologique
CRCM	Canadian Regional Climate Model
CSIRO Mk2	Commonwealth Scientific and Industrial Research Organization Mark II
DDC	Data Distribution Centre
ECHAM4	European Centre/Hamburg Model #4
EOF	Empirical Orthogonal Function
GCMs	General or Global Circulation Models
GFDL CM2x	Geophysical Fluid Dynamics Laboratory Climate Model Versions 2
GFDL R15	Geophysical Fluid Dynamics Laboratory, R-15 resolution model
GNP	Gross National Product
HadCM2/3	Hadley Coupled Models #2 and 3
HAG	Hydrological Analysis Group
IPCC	Inter-governmental Panel on Climate Change
IS92	Initial Climate Scenarios 1992
ITCZ	Inter-Tropical Convergence Zone
IVF	Index of Volumetric Fit
LARS WG	Long Ashton Research Station Weather Generator
MLR	Multiple linear regression
MM5	Mesoscale Model 5th Generation
MSLP	Mean Sea Level Pressure
NCAR	National Centre for Atmospheric Research (USA)
NCEP	National Centre for Environmental Protection
OECD	Organisation for Economic Cooperation and Development

OGCM	Ocean General Circulation Model
PBWO	Pangani Basin Water Office
PCA	Principal Components Analysis
(NCAR) PCM	(NCAR) Parallel Climate Model
PRECIS	Providing REgional Climates for Impacts Studies
RCMs	Regional Climate Models
SDSM	Statistical DownScaling Model
SRES	Special Report on Emission Scenarios
SSTs	Sea Surface Temperatures
TTT	Tropical Temperate Trough
URT	United Republic of Tanzania
UK	United Kingdom
UKMO	United Kingdom Meteorological Office
US	United States
USDA	United States Department of Agriculture
USFS	United States Forestry Services
VPO	Vice President's Office
WGEN	Weather Generator
WRED	Department of Water Resources Engineering
WRF RCM	Weather Research and Forecasting Regional Climate Model

1 INTRODUCTION

1.1 BACKGROUND

The Terms of Reference for this study were to provide modified rainfall and evaporation series for each of the selected 16 catchments in the Pangani River Basin under scenarios of climate change using statistical downscaling methods of General Circulation Models (GCMs). The modified rainfall and evaporation series is to be used for studying impacts of climate changes on river flows using the established Pitman hydrological model and a system model.

1.2 OBJECTIVES

The overall objective of the study was to examine likely impacts of climate change on river flow sequences and system yield for the Pangani Basin. The specific objective of this specialist assignment was to model scenarios of local climate variability due to global climatic change, and to use the projected climate changes to modify the “no change”, 76-year long, monthly sub-catchment rainfall sequences, and average monthly evaporation values that serve as input to the hydrological catchment model that has been configured and calibrated for the Pangani Basin. Three climate change scenarios over the Pangani Basin are required:

a) An average of regional model output or a median model.
b) A relatively dry model for the region.
c) A relatively wet model for the region.

Change projections are supposed to be sufficiently detailed to describe changes to annual precipitation, the present bi-modal distribution of monthly rainfall totals, and provide a reasonable indication of spatial variability over the basin. The spatial resolution of GCMs is considered to be too coarse to provide climate change projections, and in this regard, use of Regional Climate Models (RCMs) may be required. To provide an envelope of projected change, and to validate predictions, the results of the selected regional model need be compared with the results of at least one other model. The second set of predictions can be derived from statistical downscaling of a GCM, or from another RCM.

The Pangani Basin Water Office (PBWO) Hydrologist and members of the Pangani River Basin Flow Assessment team are expected to use the modified rainfall sequences, average monthly evaporation values, and the existing calibrated hydrological model to generate modified stream flow sequences and to assess impacts on water availability. Close communication between the two modelling groups was enhanced to ensure that the climate change modelling outputs are consistent with, and can be incorporated into, the water resources assessments.

2 LITERATURE REVIEW

2.1 INTRODUCTION

The study on likely impacts of climate change on freshwater flows in the Pangani river basin focuses on quantifying changes between current flows and simulations using scenarios of future climates. Climate scenarios are generally provided by global circulation models (GCMs) based upon the fundamental laws of physics. In this section, a review of existing GCMs, climate scenarios, downscaling techniques for GCMs output and GCM applications in Pangani basin is provided.

2.2 FUTURE CLIMATE PREDICTIONS FOR PANGANI

2.2.1 General Circulation models (GCMs)

2.2.1.1 Types

Global or General Circulation Models (GCMs) are computer models which numerically solve fundamental equations describing the conservation of mass, energy, momentum, etc. for each atmospheric gridbox, while taking into account the transfer of those quantities between gridboxes. They also consider, often in parameterized form, the physical processes within the boxes, including sources and sinks of these quantities.

The GCMs are all cartesian grid-point or spectral models which can be run at a variety of horizontal and vertical resolutions. The spectral models assume that the model domain continuously repeats itself as with earth's rotation and are up to 10 times faster than grid models particularly when complex derivatives are involved.

State-of-the-art GCMs are coupled atmosphere-ocean models (CGCMs) that simulate both atmospheric and surface and deep ocean circulations. The interface is the sea surface where the transfers of water (evaporation / precipitation) and momentum occur. Those models which simulate atmospheric circulations are the atmosphere GCMs (AGCMs) while GCMs simulating the oceanic circulations are ocean GCMs (OGCMs).

2.2.1.2 Available CGCMs

Currently, there exists generally a number of GCMs broadly falling under atmosphere, ocean or coupled GCM categories. Most of widely used GCMs in the assessments of impacts of climate changes are the coupled GCMs which provide projections of global climates under scenarios of changing background factors like concentrations of greenhouse gases. Widely used coupled GCMs in climate change studies (Table 2.1) include:

i) The UK Hadley Centre for Climate Prediction and Research, Coupled models #2 and 3 (HadCM2/3)

ii) The Canadian Centre for Climate Modelling and Analysis Versions 1 and 2 (CGCM1/2)
iii) The German Climate Research Centre, European Centre/Hamburg, Model #4 (ECHAM4)
iv) The Australian Commonwealth Scientific and Industrial Research Organization, Model #2b (CSIRO Mk2b)
v) The American US Geophysical Fluid Dynamics Laboratory, R-15 resolution model (GFDL R15) and
vi) The Japanese Centre for Climate Research Studies (CCSR98)

Table 2.1: Information of available coupled GCMs.

GCM	CGCM1	CGCM2	HadCM2	ECHAM4	CCSR98	CSIROMk2b	GFDL-R15	GFDL-CM2.1
GCM Type	Spectral T32	Spectral T32	Finite Grid	Spectral T42	Spectral T21	Spectral R21	Spectral R15	Finite Grid
AGCM Resolution °lat×°long	3.75×3.75	3.75×3.75	2.5×3.75	2.8×2.8	5.6×5.6	3.2×5.6	4.5×7.5	2×2.5
AGCM Number of vertical levels	10	10	19	19	20	9	9	24
Global grid: number of lat×long boxes	48×96	48×96	73×96	128×64	64×32	64×54	48×40	90×144
OGCM Resolution °lat×°long	1.8×1.8	1.8×1.8	2.5×3.75	2.8×2.8	2.8×2.8	3.2×5.6	4.5×3.7	1×1
OGCM Number of vertical levels	29	29	20	11	17	21	12	50
Flux correction	Yes		Yes	Yes	Yes	Yes	Yes	No

2.2.1.3 Emission scenarios

There are mainly 3 types of climate change scenarios, synthetic (arbitrary) scenarios, analogue scenarios and scenarios from GCM. Synthetic scenarios are the simplest climate scenarios in which a historical record for a particular climate variable is simply perturbed by an arbitrary amount. Analogue scenarios are constructed by identifying a recorded climate regime which may resemble the future climate anticipated for a particular site or region. These recorded climates may be identified in the long observational record at a site (*temporal analogues*) or be from other geographical locations (*spatial analogues*).

Scenarios from GCM are plausible representations of the future that are consistent with assumptions about future emissions of greenhouse gases and other pollutants and with our understanding of the effect of increased atmospheric concentrations of these gases on global climate. A range of scenarios can be used to identify the sensitivity of an exposure unit to climate change and to help policy makers decide on appropriate policy responses. It is important to emphasise that climate scenarios are not predictions. A climate scenario is a plausible indication of what the future could be like over decades or centuries, given a specific set of assumptions. These assumptions include future trends in energy demand, emissions of greenhouse gases, land use change as well as assumptions about the behaviour of the climate system over long time scales. It is largely the uncertainty surrounding these assumptions that determines the range of possible scenarios.

2.2.1.3.1 IS92 emission scenarios

In order to determine how climate may change in the future we need to know how the concentrations of those atmospheric components that affect the Earth's energy balance may change. Gases such as water vapour, carbon dioxide, methane and nitrous oxide (the greenhouse gases) absorb long-wave (heat) radiation emitted from the Earth's surface and re-emit this energy, ultimately resulting in raised surface temperatures. Whilst these greenhouse gases occur naturally, human activities since the beginning of the industrial revolution have resulted in large increases in the atmospheric concentrations of these gases and it is now widely accepted that this has affected global climate. This has led to a release of six initial climate scenarios, the IS92 (Leggett *et al*., 1992). These six emissions scenarios reflected the large uncertainty associated with, for example, the evolution of population and economic growth, technological advances, technology transfer and responses to environmental, economic or institutional constraints. They are IS92a, IS92b, IS92c, IS92d, IS92e and IS92f and are considered equally likely.

IS92a
A middle of the range scenario in which population rises to 11.3 billion by 2100, economic growth averages 2.3% $year^{-1}$ between 1990 and 2100 and a mix of conventional and renewable energy sources are used. Only those emissions controls internationally agreed upon and national policies enacted into law, e.g., London Amendments to the Montreal Protocol, are included.

IS92b
Population rises to 11.3 billion by 2100 and the current emissions control policies are enlarged to include stated policies beyond those legally adopted, e.g., all CO_2 commitments of OECD member countries are included along with an assumption of world-wide ratification and compliance with the amended Montreal Protocol.

IS92c
Economic growth averages 1.2% year between 1990 and 2100 and population is forecast to be 6.4 billion by 2100, with population decreasing in the 21st century. As well as assuming lower growth in GNP per capita than IS92a and IS92b, low oil and gas resource availability results in higher prices, which promote the expansion of nuclear and renewable energy. Lower population growth results in slower deforestation rates.

IS92d
Like IS92c, this is a low-emission scenario, but it is more optimistic than IS92c. The trend is towards increasing environmental protection but only actions that could be taken due to concerns about local or regional air pollution and waste disposal are included. Population is forecast to be 6.4 billion by 2100 and would be associated with lower natality, falling below the replacement rate late in the 21st century, due, for example, to improvements in per capita income or increased family planning. Low fossil fuel resource availability means that there is greater market penetration of renewable energy and safe nuclear power. A 30% environmental surcharge on fossil energy use is levied to meet the costs of more stringent local pollution controls. Greater well-being is assumed to lead to voluntary actions to halt deforestation, to adopt CFC substitutes with no radiative or other adverse effects and to recover and efficiently use the methane from coal mines and land fills.

IS92e
Results in the highest CO_2 emissions. Economic growth averages 3% year^{-1}, between 1990 and 2100 and the population is forecast to reach 11.3 billion by 2100. Fossil resources are plentiful but, due to assumed improvements in living standards, environmental surcharges are imposed on their use. Nuclear energy is phased out by 2075 and, although CFC substitute assumptions are the same as those of IS92d, the plentiful fossil fuel resources discourage the additional used of coal mine methane for energy supply. Deforestation proceeds at the same pace as IS92a.

IS92f
Falls below IS92e, has high population growth (17.6 billion by 2100), but lower assumptions of improvements in GNP per capita than IS92a. Other assumptions are high fossil fuel resource availability, increasing costs of nuclear power and less improvement in renewable energy technologies and costs.

Fig 2.1 illustrates the global-mean temperature change associated with the six IS92 scenarios.

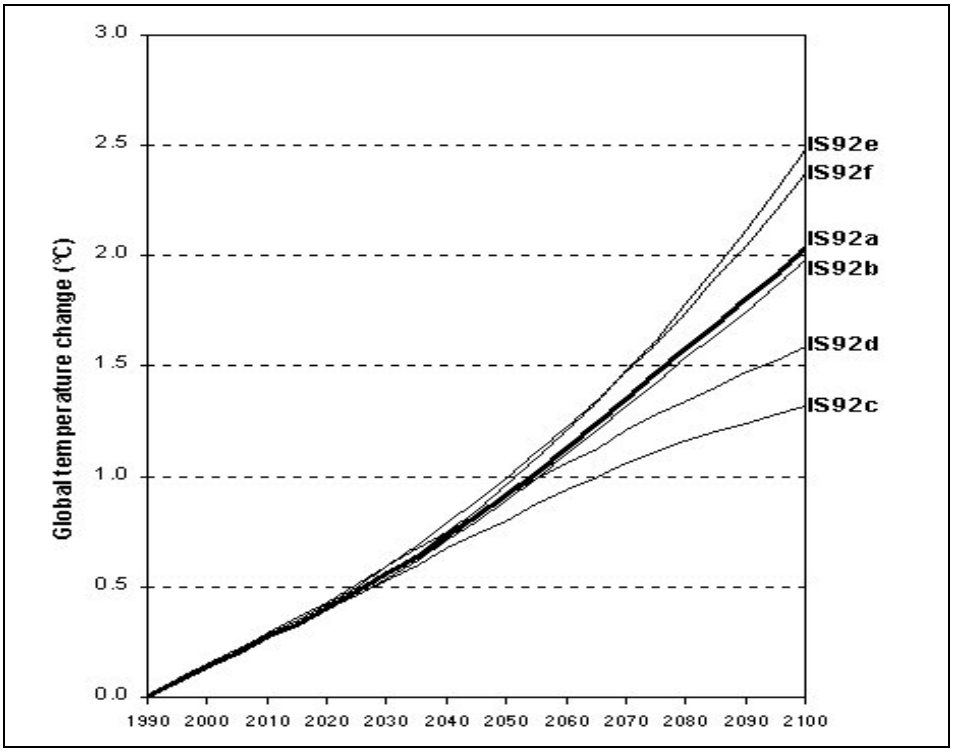

Fig 2.1: Global-mean temperature change (°C) associated with the six IS92 emissions scenarios.

2.2.1.3.2 SRES emission scenarios

There are, naturally, inherent uncertainties in determining how atmospheric composition may change in the future. This is attributed by assumptions about how both the natural and anthropogenic emissions of these greenhouse gases will change which, in turn, is dependent on assumptions regarding population growth, economic activity, energy use, land use change, etc. Thus, with time, it

became necessary to revise the IS92 scenarios and this process gave the new set of climate scenarios, the SRES emission scenarios (IPCC, 2001).

The IPCC Special Report on Emission Scenarios (SRES; Nakicenovic *et al*., 2000) details four storylines, narratives of qualitative (e.g., political, social, cultural and educational conditions) emissions drivers. The SRES emissions scenarios are the quantitative interpretations of these qualitative storylines. The six general marker SRES climate scenarios (Fig 2.2) are A1FI, A1T and A1B from the A1 family, and A2, B1 and B2.

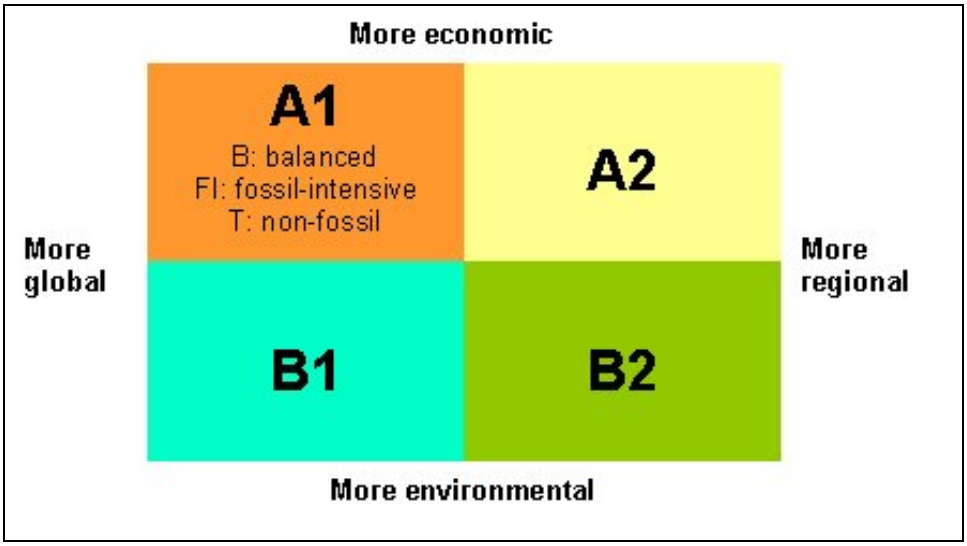

Fig 2.2: A schematic representation of the SRES scenario family. The A1 and A2 families have a more economic focus than B1 and B2, which are more environmental, whilst the focus of A1 and B1 is more global compared to the more regional A2 and B2.

A1FI, A1T and A1B

The A1 storyline and scenario family describes a future world of very rapid economic growth, global population that peaks in mid-century and declines thereafter, and the rapid introduction of new and more efficient technologies. Major underlying themes are convergence among regions, capacity-building, and increased cultural and social interactions, with a substantial reduction in regional differences in per capita income. The A1 scenario family develops into three groups that describe alternative directions of technological change in the energy system. The three A1 groups are distinguished by their technological emphasis: fossil intensive (A1FI), non-fossil energy sources (A1T), or a balance across all sources (A1B; where balanced is defined as not relying too heavily on one particular energy source, on the assumption that similar improvement rates apply to all energy supply and end use technologies).

A2

The A2 storyline and scenario family describes a very heterogeneous world. The underlying theme is self-reliance and preservation of local identities. Fertility patterns across regions converge very slowly, which results in continuously increasing population. Economic development is primarily regionally oriented and per capita economic growth and technological change more fragmented and slower than other storylines.

B1
The B1 storyline and scenario family describes a convergent world with the same global population that peaks in mid-century and declines thereafter, as in the A1 storyline, but with rapid change in economic structures toward a service and information economy, with reductions in material intensity and the introduction of clean and resource-efficient technologies. The emphasis is on global solutions to economic, social and environmental sustainability, including improved equity, but without additional climate initiatives.

B2
The B2 storyline and scenario family describes a world in which the emphasis is on local solutions to economic, social and environmental sustainability. It is a world with continuously increasing global population, at a rate lower than A2, intermediate levels of economic development, and less rapid and more diverse technological change than in the B1 and A1 storylines. While the scenario is also oriented towards environmental protection and social equity, it focuses on local and regional levels.

Changes in global-mean temperature associated with each of the six marker scenarios are illustrated in Fig 2.3. The response of global-mean temperature to the different emissions scenarios can be determined by using a relatively simple upwelling diffusion energy balance (UD/EB) climate model, such as the one developed by Wigley and Raper (1992). This model distinguishes between land and ocean and between the hemispheres, but simulates only the underlying signal in response to external forcing and not the variability.

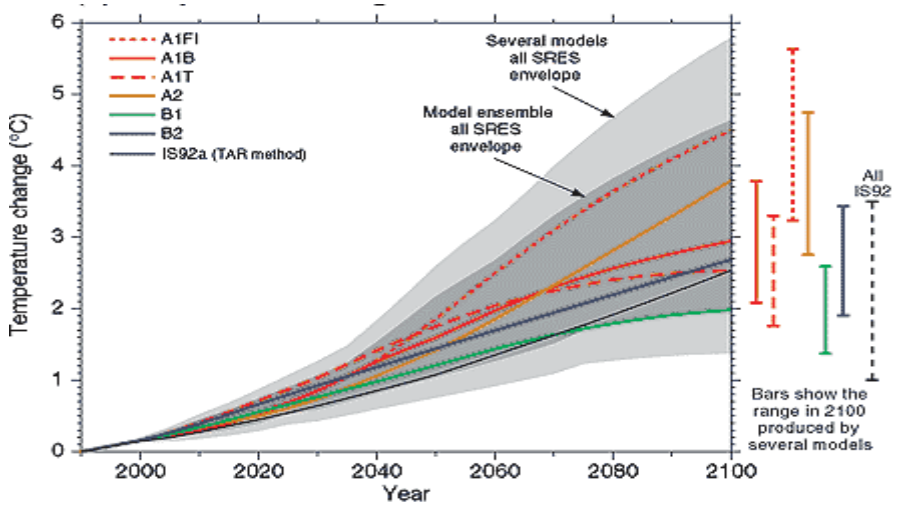

Fig 2.3: Global-mean temperature change (°C) associated with the six SRES marker scenarios, A1FI, A1T, A1B, A2, B1 and B2.

2.2.1.4 Selection and application of GCM climate change scenarios

2.2.1.4.1 Selection of GCM climate change scenarios

Although there is increasing confidence among atmospheric scientists that increased atmospheric greenhouse gas concentrations will increase global temperatures, there is much less confidence in estimates of how the climate will change at a regional scale. However, it is precisely at this regional or local level

(e.g. at the scale of a farm, a river catchment or even an individual organism) that climate change will be felt. Since no method yet exists of providing confident predictions of climate change at these scales, an alternative approach is to specify a number of plausible future climate scenarios.

The choice of climate scenarios among the existing many (Table 2.2) and related non-climatic scenarios is important because it can determine the outcome of a climate impact assessment. Extreme scenarios can produce extreme impacts; moderate scenarios may produce more modest effects. It follows that the selection of scenarios can also be controversial, unless the fundamental uncertainties inherent in future projections are properly addressed in the impact analysis.

The three recommended future time periods (IPCC, 2001) for climate change impact analysis are 2010-2039 (representing the 2020s), 2040-2069 (the 2050s) and 2070-2099 (the 2080s). Since there is little confidence on daily data derived from GCMs, monthly data are usually used.

Table 2.2: Available coupled GCMs SRES scenario runs.

Centre	Acronym	Model	SRES Scenario Runs					
Max Planck Institute für Meteorologie	MPIfM	ECHAM4/OPYC3				A2		B2
Hadley Centre for Climate Prediction and Research	HCCPR	HADCM3		A1FI		A2 A2b A2c	B1	B2 B2b
Australia's Commonwealth Scientific and Industrial Research Organisation	CSIRO	CSIRO-Mk2	A1			A2	B1	B2
National Centre for Atmospheric Research	NCAR	NCAR-CSM				A2		
		NCAR-PCM	A1B			A2		B2
Geophysical Fluid Dynamics Laboratory	GFDL	R30				A2		B2
		CM2.1	A1	A1F1		A2	B1	B2
Canadian Center for Climate Modelling and Analysis	CCCma	CGCM2				A2 A2b A2c		B2 B2b B2c
Center for Climate System Research (CCSR) National Institute for Environmental Studies (NIES)	CCSR / NIES	CCSR/NIES AGCM + CCSR OGCM	A1	A1FI	A1T	A2	B1	B2

2.2.1.4.2 Application of GCM climate change scenarios

The application of GCM outputs in impact assessments has normally involved the use of the *best guess* scenario. This practice of using the *best guess* climate scenarios in impact assessments may increase unreliability of future predictions resulting from inherent GCM uncertainties in future greenhouse gas and aerosol emissions, global climate sensitivity and regional climate changes. It is strongly recommended that multiple scenarios (GCM ensembles) in any impact assessments to include almost all possible future climates.

The output from GCMs is not generally of a sufficient resolution or reliability to be applied directly to represent present-day climate or consequently future climate conditions. It is a standard practice to use observed data representing the current baseline period (e.g. 1961-1990) and to apply changes derived from GCM information (i.e. the scenarios) to these observed data. In general, these GCM-derived scenarios are for the single grid box, which contains the location of the study area. However, GCMs can display a large difference in their estimates of climate change, particularly for variables like precipitation, at the regional level. Therefore, although most impacts studies have followed this approach, lack of confidence in regional estimates of climate change from GCMs has led to the suggestion that the minimum effective spatial resolution should be defined by at least four, and possibly more GCM grid boxes (von Storch *et al*., 1993).

If GCM ensembles are used, the application of scenarios to impact assessments is a straightforward process. Either an observed time series is perturbed by monthly scenario changes, or a stochastic weather generator is used to obtain daily data for a particular scenario. A scenario of future climate is obtained by adjusting the baseline observations by the difference (or ratio) between period-averaged results for the GCM experiment (usually 30 year periods) and the simulated baseline period (1961 –1990). To obtain a monthly series representing the 2050s, for example, the observed monthly rainfall series in the 1961 – 1990 baseline period is rescaled through multiplication by the percentage change in rainfall between the baseline and future periods. If this change for April monthly rainfall amounts is 0.9 (a 10% decrease), the series of April monthly rainfall amounts in the 2050s is simply that in 1961 – 1990 period multiplied by 0.9.

Since all scenarios are calculated with respect to a particular reference period (currently 1961-1990), therefore, the scenarios should be applied only to observed data representing that period. Moreover, there are some caveats of which scenario users need to be aware. When applying GCM-derived scenario changes to an observed time series, it is assumed that the variables match.

2.2.2 Downscaling of GCM outputs

For many climate change studies, scenarios of climate change derived directly from GCM output may not be of sufficient spatial or temporal resolution. The spatial resolution of GCMs means that the representation of, for example, orography and land surface characteristics, is much simplified compared to reality. This results in a consequent loss of some of the characteristics, which may have important influences on regional climate (e.g. lakes system in East Africa). The need for detailed site or regional scenarios of climate change for impacts studies has existed for a number of years (Lamb, 1987; Cohen, 1990). This need has resulted in the development of a number of methodologies for deriving such information, generally from GCMs that, despite their shortcomings at finer

resolution, are recognized as the best available method for determining internally-consistent scenarios of future climate (Hulme *et al*., 1990; Giorgi and Mearns, 1991; Robock *et al*., 1993). These methodologies are termed 'downscaling.' Downscaling techniques have been designed to bridge the gap between the information that the climate modeling community can currently provide and that required by the impacts research community (Wilby and Wigley, 1997). Downscaling techniques can be divided into spatial and temporal classes.

2.2.2.1 Spatial downscaling

Spatial downscaling refers to the techniques used to derive finer resolution climate information from coarser resolution (usually 250 – 600 km) GCM output (Fig 2.4). The fundamental bases of spatial downscaling are the assumptions that it will be possible to determine significant relationships between local and large-scale climate (Fig 2.5) and that these relationships will remain valid under future climate conditions. This allows meaningful site-scale information to be determined from large-scale GCM information. Spatial downscaling may be able to incorporate some of regional climate controls and therefore add value to coarse-scale GCM output in some areas particularly those with strong local climatic influences such as topography and inland lakes.

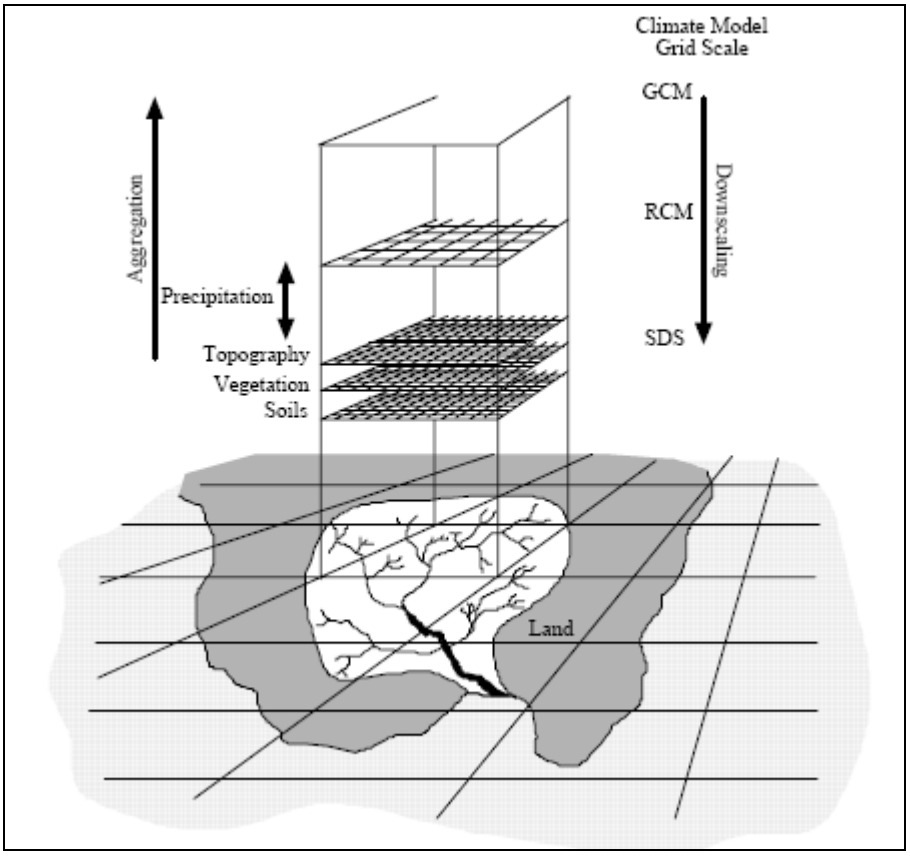

Fig 2.4: A schematic illustration of general spatial downscaling process (Source: SDSM Manual).

There are a number of general recommendations for spatial downscaling, which facilitate the process and include:

i) The GCM used for spatial downscaling should reasonably simulate atmospheric features controlling local climate;
ii) The downscaling technique should use climate variables that does not exhibit large sub-grid scale variations; and,
iii) The climatic variables used in the downscaling process should ideally be primary model variables (direct model outputs).

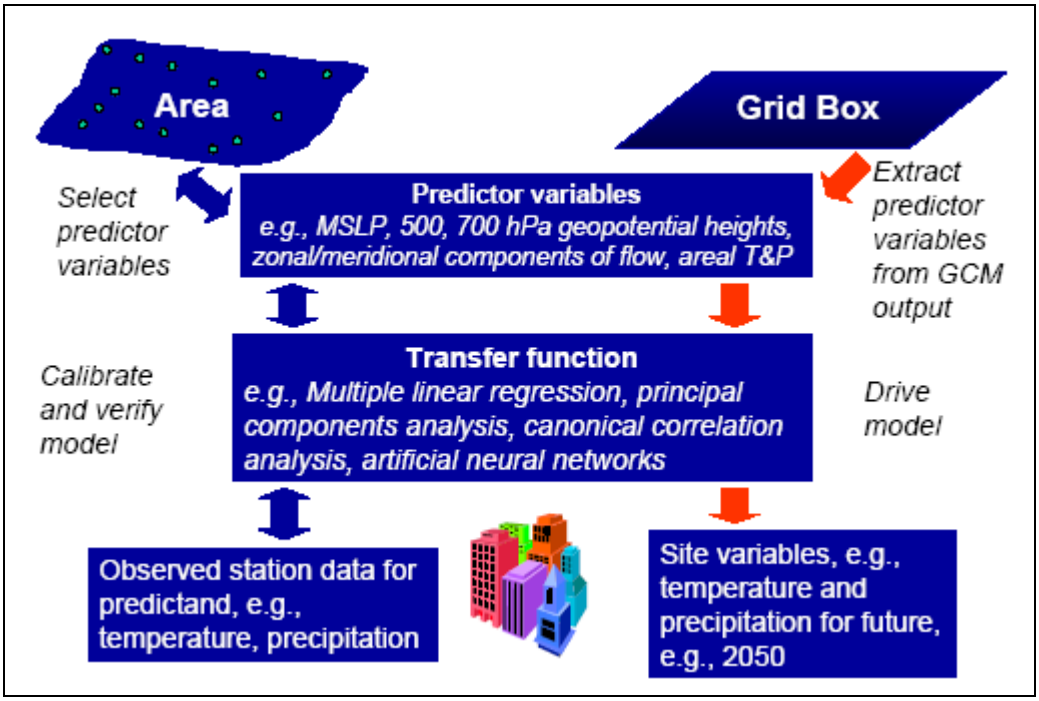

Fig 2.5: The transfer approach to spatial downscaling (Source: http://www.ceaa-acee.gc.ca/015/001/004/PDF/Figure15_e.pdf).

2.2.2.1.1 Statistical downscaling

Statistical downscaling techniques use empirical relationships between large-scale atmospheric data (e.g. GCM scale climate data) and observed local climate data to compute finer sub-grid or station climatic changes from large-scale GCM outputs. The statistical downscaling process involves the following:

i) defining statistical relationships based on observed data; and,
ii) using models based on established statistical relationships to study the impacts of climate change.

To effectively define statistical relationships between local-scale and large-scale climatic variables, it is important to identify the large-scale climatic predictor variables that influence the local climate to be used in the transfer function (Fig 2.5). The predictors are required to be (Wilby *et al*., 2001):

i) physically and conceptually sensible to site predictand;
ii) strongly and consistently correlated with the predictand;
iii) readily and easily available from archives of observed data and GCM outputs; and,

iv) accurately modelled by GCMs.

The correlation analysis can preliminarily be used to investigate the existence or non-existence of the relationships between local-scale and large-scale climatic variables (variable screening). This procedure will retain those climatic predictor variables that strongly correlate with the predictand. The normalised predictand and predictor variables are used to establish the transfer functions during model calibration and verification. The normalisation, which reduced GCM bias, facilitates the use of GCM-derived climate change scenarios are usually expressed as changes with respect to the baseline period (currently, 1961 – 1990). There exist several methods for estimating the transfer functions including multiple linear regression, principal components analysis, singular value decomposition, etc). However, each method has its own weaknesses, which should be considered during the model development process.

The determination of model performance is rather subjective and usually depends on data availability and local climatic conditions. Whilst it can be easier to downscale statistically GCM outputs on a relatively level terrain, model performance in mountainous locations can sometimes be poor if selected variables do not capture the existing local-large-scale variables relationships. The calibrated and verified models are then driven by GCM outputs for the concurrent period as observed data to assess the ability of GCM to simulate the current climate at that particular location. Once the models have been calibrated and verified using observed data and ability of GCM simulation assessed, GCM output of predictor variables for future climates are then used to drive the model to provide climate change scenarios during the study of the impacts of climate changes.

The main advantages of statistical downscaling techniques are the relative ease of application, adaptability for rapid climate change impacts assessment and suitability for site-specific scenario development. However, their main weaknesses are related to their low percentages of explained variances in observed series particularly when specialist knowledge is missing, requirement of large amounts of observational data and sometimes produced scenarios are insensitive of future climatic forcings.

2.2.2.1.2 Dynamical downscaling

Dynamical downscaling techniques are based on physical or dynamical links between the climate at the large scale and at smaller scales. It involves nesting of high-resolution regional climate model (RCM) within a coarser resolution driving GCM. It is usually implemented by running either a full GCM at varying resolution across the globe with the highest resolution over the study area or a RCM using GCM results as its boundary conditions to simulate climate features and physical processes in much greater detail for such a limited study area. However, the nesting is a one-way RCM – GCM process with no feedbacks from RCM to GCM.

The main advantage of RCMs is that they can resolve local scale atmospheric features better than GCMs. They are, however, computationally demanding both in simulation time and resources while generated scenarios are sensitive to the choice of initial boundary conditions. Moreover, the grid spacing of most RCMs is currently limited to about 50 km although some go down to 20 km. This limits the

amount of details that can be available for impacts assessments and therefore render them unsuitable for smaller catchments unless subsequent downscaling by other techniques is applied to RCM outputs.

Some examples of RCMs include PRECIS, Canadian RCM (CRCM), MM5, GESIMA and Weather Research and Forecasting RCM (WRF RCM).

2.2.2.2 Temporal downscaling

Temporal downscaling refers to the derivation of fine-scale temporal data from coarser-scale temporal information (e.g. daily data from monthly or seasonal information). Its main application is in scenario studies, particularly for the derivation of daily scenario data from monthly or seasonal scenario information. The simplest method for obtaining daily data for a particular climate change scenario is to apply the monthly or seasonal changes to a historical daily weather record for a particular station. However, this method maintains the current observed climate variability and the same sequences of, for example, wet and dry days and hot and cold spells.

There is always one time series available for each scenario, which limits the type of analyses for which the daily data can be used. Stochastic weather generators, which generate time series of artificial weather data with the same statistical characteristics as the observations for the station, are used to overcome this deficiency. Their main assumption is that the statistical correlations between the climate variables, derived from observed data, are valid under a changed climate.

During the calibration process, the model creates a set of parameters that statistically describe characteristics of the climate at that particular site the site. The downscaling process then modifies this set of parameters through perturbation of the appropriate parameters. Climate change scenarios are generated using perturbed parameters. Their main advantage is that they can generate a number of series of unlimited length with exactly same statistics as observed climate and are therefore suitable for risk analysis. Their main weakness is related to arbitrary adjustment of parameters to simulate future climates and their station-specific designed use.

Some examples of stochastic weather generators include Long Ashton Research Station Weather Generator (LARS WG), Richardson Weather GENerator (WGEN) and USDA ARS-USFS CLImate GENerator (CLIGEN).

3 DATA AND METHODOLOGY

3.1 INTRODUCTION

This section describes the data sets and methodology used in the study. The data are observed rainfall and evaporation series and GCM simulated climatic variables. The description includes their sources, quality and period of available data and construction of such catchment series of rainfall and climatic variables (evaporation, temperature, solar radiation, relative humidity, wind speed, etc).

3.2 DATA

3.2.1 Rainfall and climatic data

Monthly rainfall data for 122 stations in the Pangani river basin were obtained from the Hydrological Analysis Group (HAG) of the Pangani Basin Management Project and the Department of Water Resources Engineering (WRED) of the University of Dar es Salaam. The spatial distribution of the stations in the basin (Fig 3.1) is non-uniform with high density in the Usambara Mountains, Mount Kilimanjaro and Mount Meru. This is attributed by the development of settlements in these areas compared to other parts of the basin.

Acquired rainfall records were, however, of variable quality and record length. This necessitated their selections to retain a few quality and considerably long records for the study. Using criteria of data availability in the 1961-2000 period, less than 15% missing in the 1961-2000 period and neighbourhood resemblance (high cross-correlations), 65 records were retained for the study.

The available climatic data (evaporation, temperature, solar radiation, relative humidity, wind speed, etc) were obtained from HAG. The spatial variation of the recording stations was, however, very poor.

Climate change scenarios are developed for 16 selected catchments (Fig 3.1) and therefore catchment rather than stations series of rainfall and climatic variables are used. The HAG used selected series to construct series of catchment rainfall and evaporation for the period 1951-2005. The catchment rainfall time series generally span the period 1920 – 2005, expressed in percentages of mean annual rainfall calculated over the same period, were made available to the consultant team for this study.

3.2.2 Re-analysis data

The daily NCEP/NCAR re-analysis data were obtained from the Canadian Institute for Climate Studies (CICS) Canadian Climate Impacts Scenarios (CCIS) Project website (http://www.cics.uvic.ca/scenarios/sdsm/select.cgi). The data have been standardised with respect to mean and standard deviations of the 1961-1990 period and re-grided to approximate grids of the HadCM3 GCM (2.5° lat ×

3.75° long). The time period of availability is from January 1961 to December 2001.

Monthly series of NCEP/NCAR re-analysis data were obtained online from the project website[1]. The data is available at the spatial grids of 2.5° latitude by 2.5° longitude and spans the period from January 1948 to present. The data sets are separated into seven sections describing pressure level, surface, surface fluxes, other fluxes, tropopause[2], derived data and spectral coefficients. Data for a number of surface and upper troposphere variables are available.

Fig 3.1: Location of catchments established and made available for the study.

3.2.3 GCM output data

Many GCM experiments are now available for use in climate change studies. The experiments available reflect state-of-the-art model experiments and provide a representative range of results from different GCMs. The available GCM outputs can be freely accessed and downloaded from the Data Distribution Centre

[1] Website: http://www.cdc.noaa.gov/cdc/reanalysis

[2] Tropopause *is the boundary between the troposphere and stratosphere, characterised by an abrupt change in temperature lapse rate (temperature decreases with height in the troposphere, but increase or remain constant with height in the stratosphere)*

(DDC[3]) of the Intergovernmental Panel of Climate Change (IPCC). The outputs for the seven widely used coupled GCMs (Table 3.1) are available for both IS92 and SRES emission scenarios.

The data set for each GCM experiment consists of monthly values for eight surface variables: precipitation rate, mean sea level pressure, solar radiation, mean air temperature, dew point temperature (or vapour pressure or relative humidity), minimum air temperature, maximum air temperature and 10 m wind speed (Table 3.2). It should be noted, however, that if a particular variable is unavailable in the list, it might have been replaced with a similar variable (e.g. relative humidity replacing dew point temperature). Other optional data are available and include geopotential heights (hPa), relative humidity, air temperature, winds (direction, zonal and meridional) at various tropospheric levels.

The GCM outputs are available at the daily and monthly timescales. Due to inherent uncertainties with daily outputs, only monthly series were downloaded. The available GCM output data span mainly three periods. Outputs of CGCM2 span the period 1900 – 2100, those of HadCM2/3 and CSIRO Mk2 the period 1961 – 2100, while those of ECHAM4/OPYC3 extend in the 1990 – 2100 period. For comparable results between various GCMs, the period 1961 – 2099 is used and consequently outputs of ECHAM4/OPYC3 are excluded in this study. Output of the GFDL CM2.1 span the period 1900-2099.

The scenarios data available from the DDC are at the global scale and users accessing this Web site must download the complete global fields for each experiment. However, data for HadCM3 and CGCM1 experiments were downloaded from CCIS Project website. Unlike downloading from IPCC DDC, data from the CCIS source were downloaded for particular gridboxes in areas in which oceanic and atmospheric variables have influences on Pangani rainfall and climate (Fig 3.2).

3.3 METHODOLOGY

3.3.1 Selection of downscaling method

The selection between statistical and dynamical downscaling techniques is carried out by consideration of limiting time (which is 3 months) and simulation resources for the study. For a rapid assessment of climate change over spatially small catchments like those selected for this study, statistical downscaling methods are the most preferred ones. They are computationally less demanding in terms of simulation resources (time, computational resources – electricity, computers, etc) and provide information at the individual stations. Although dynamical downscaling techniques can provide better simulations of local conditions, their current coarse spatial scale (usually ~ 50 km), demanding simulation resources (simulation time – some months, reliable electricity, powerful computers) and configuration of boundary conditions make them unsuitable for this rapid assessment study.

[3] Website: http://ipcc-ddc.cru.uea.ac.uk)

Table 3.1: Available coupled GCMs SRES A2 scenario runs outputs.

Parameter Description	**unit**	ECHAM4/OPYC3	HADCM3	CSIRO-Mk2	NCAR-CSM	NCAR-PCM	R30	CGCM2	GFDL CM2.1
2m mean surface air temperature	K	X	X	X	_			X	X
2m mean maximum air temperature	K	X	X	X	_			X	X
2m mean minimum air temperature	K	X	X	X	_			X	X
total precipitation	mm/d	X	X	X	_			X	X
total incident solar radiation	W/m^2	X	X	X	_			X	X
mean scalar wind speed	m/s	X	X	X	_			X	X
Humidity	%	X	X		_			X	X
mean sea level pressure	hPa	X	X	X				X	X
global mean sea level change (thermal expansion)	mm/y								
optional data									
daily mean temperature variance	K								
daily precipitation variance	K							X	
surface skin temperature / SST	K	X		X				X	X
soil moisture(content)	mm	X	X	X				X	X
large scale precipitation (rain/snow)	mm/d	X							
convective precipitation (rain/snow)	mm/d	X		X					X
snow cover									X
snow melt	mm/d	X							X
snow depth (snow amount)	kg/m^2	X	X	X				X	X
850 hPa height	gpm	X	X						X
500 hPa height	gpm	X	X					X	X
200 hPa height	gpm	X	X						X
850 hPa height variance	gpm								
500 hPa height variance	gpm							X	
200 hPa height variance	gpm								
850 hPa temperature	K	X	X	X					X
500 hPa temperature	K	X	X	X					X
200 hPa temperature	K	X	X	X					X
850 hPa rel. humidity	%	X	X	X					X
500 hPa rel. humidity	%	X	X	X					X
200 hPa rel. humidity	%	X	X	X					X
850 hPa u-wind	m/s	X		X					X
500 hPa u-wind	m/s	X		X					X
200 hPa u-wind	m/s	X		X				X	X
850 hPa v-wind	m/s	X		X					X
500 hPa v-wind	m/s	X		X					X
200 hPa v-wind	m/s	X		X				X	X

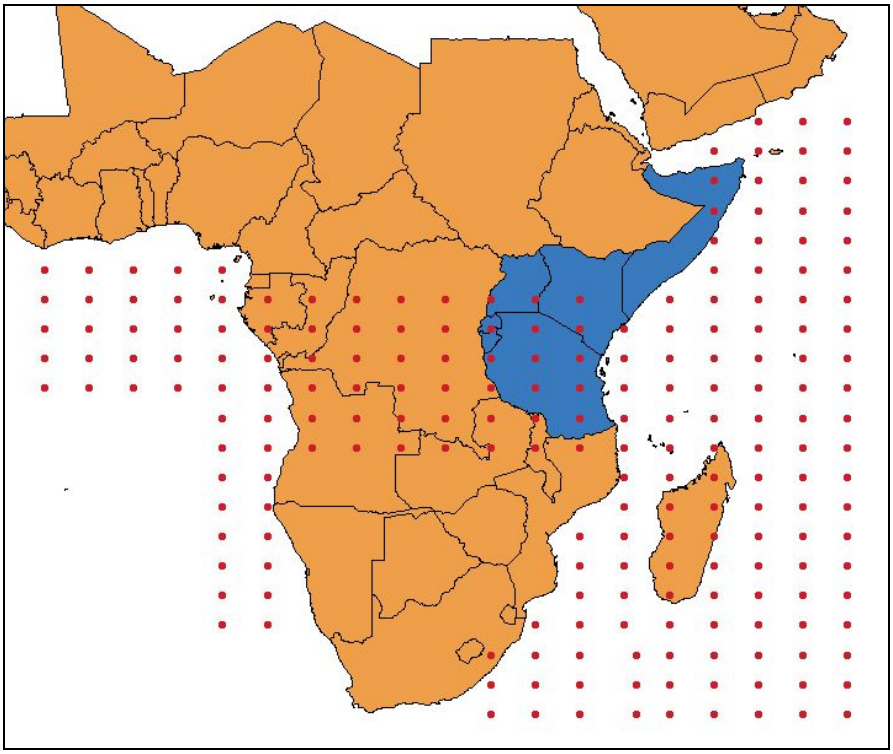

Fig 3.2: Location of gridboxes where oceanic and atmospheric variables have an influence on Pangani rainfall.

The time limitation of RCMs is illustrated by the long required time by PRECIS RCM to simulate future perturbed climates. For moderately fast personal computers (PCs) (UNIX operating system, at least 512 Mb of RAM, storage size of 60 Gb or more, minimum preferred speed of 2 GHz and a tape drive for external storage), it takes 6 weeks to complete a 10 years simulation while it requires 5-6 months to complete a 30 years simulation.

Unlike PRECIS running on PCs, most of the RCMs like the Canadian RCM (CRCM) and MM5 mentioned in Section 2.2.2.1.2 usually run in large computing installations and therefore cannot be run on PCs, which are readily available to and currently used by many researches. Their requirements of extensive computing resources including fast computers and a considerable amount of effort from experienced climate modelers make them inappropriate in many developing countries like Tanzania.

The suitability of current RCMs for smaller catchments like some of Pangani is limited by spatial coarseness of the RCM grids. This is illustrated by the 50 km $\times$ 50 km grid size of PRECIS model, the grid size currently used in simulation. Although a much finer grid size of 10 km $\times$ 10 km that will closely approach the observation grids is planned in the future, the PRECIS model minimum grid size current in use is the 25 km $\times$ 25 km, still too coarse to resolve sub-grid processes for the Pangani catchments.

As interfacing RCMs with a range of GCMs is complicated and, RCM data requirements, output data and computing resources to run RCM with a number of GCMs are substantial, currently most of RCMs are mainly used to downscale

outputs of the GCMs that are developed by the developer of RCM. This is true for PRECIS, which is bounded by the Hadley HadCMx GCMs and consequently downscales the outputs of the Hadley developed GCMs, although efforts are underway to possibly use other GCMs. Similarly, MM5 is bounded by GFDL CMx while CRCM's boundary conditions are from the CCCMa's CGCMx. Since RCMs are dependent on the realism of the background GCMs driving them, the usefulness of their predictions is strongly influenced by the correctness of representation of regional climates. The PRECIS RCM overestimates rainfall in much of Southern Africa (PRECIS Handbook, 2004) is an illustration of the need to evaluate the suitability of the driving GCM in reproducing the regional climates before applying RCMs.

Therefore, statistical downscaling methods will be used for construction of climate change scenarios in the Pangani River basin.

3.3.2 Development of rainfall/evaporation prediction models

3.3.2.1 Selection of climatic predictors and influencing regions

The development of prediction models for rainfall and evaporation (or air temperature, wind speed) will use findings of past studies on the relationships between local Pangani climates and large-scale climatic variables. Past studies have indicated that rainfall in the basin is affected by both atmospheric (surface and upper air) and oceanic (surface) variables. Of the atmospheric variables, the zonal (u-) and meridional (v-) winds, geopotential heights have been linked with rainfall variations in the basin. Although relative humidity (rhum) has not been widely used in the past studies, it is among the useful atmospheric variables of water content related to sources of moisture that is transported by winds to the basin. Oceanic variables that have shown influence on Pangani climate are the SSTs although some studies have indicated the influence of MSLP. Owing to strong relationship between SSTs and MSLP and the latter being among the GCM outputs, MSLP is used as an oceanic predictor in this study.

Since different past studies have used atmospheric and oceanic predictors from basins of variable sizes and obtained variable prediction model efficiencies for whole region, this study is re-establishing the spatial extent of oceanic and atmospheric basins which have significant influence on Pangani climate. The procedure therefore involves the following

i) Selection of atmospheric and oceanic variables for analysis (preference is on u- and v-winds, rhum, geopot and MSLP).
ii) Selection of oceanic and atmospheric basins (from past studies they include whole Indian Ocean west of 90°E between 17°N and 35°S, land area between 12.5°N and 12.5°S and Atlantic Ocean east of 15°W between 12.5°N and 25°S).
iii) Computation of correlations between catchment rainfall and climatic (evaporation, temperature, wind speed, etc) series and gridbox climatic variables in the selected oceano-atmospheric basins. The correlations are between monthly series and for three periods, 1961-2001, 1961-1979 and 1980-2001. This will provide the best-fit period for model development.
iv) Gridboxes with highest correlations with catchment variables will be isolated and marked as influential basins. These gridboxes will be used to

compute areal monthly averages of climatic predictors for further modelling.

v) Oceanic and atmospheric variables within the influential basins providing highest correlations with catchment variables will be identified and isolated.

3.3.2.2 Establishment of rainfall/evaporation prediction models

The development of statistical models for assessing the impacts of future climates on Pangani climate is carried out using observed rainfall and evaporation (or its estimating variables like temperature) and NCEP/NCAR re-analyses. The multiple linear regression (MLR) models are used in statistical downscaling in this study and the process involves model calibration, verification and application.

3.3.2.2.1 MLR model calibration

The general form of the adopted MLR model is

$$Y = a_0 + a_1X_1 + a_2X_2 + ... + a_nX_n \quad (3.1)$$

where Y is the predictand dependent on "semi" independent predictors X_i's and ai are model parameters estimated during calibration.

The model calibration process involves the selection of predictors which are appropriate for model development in which the prior knowledge of predictor-predictand is essential in predictors screening. This is facilitated by cross correlation analysis between predictand variables and potential predictor variables retaining those predictors highly correlated with the predictands. The number of predictors will be optimised to avoid the over-fitting (due to collinearity, that is, too many predictors in the model that are highly correlated) and under-fitting (too few predictors) problems and consequential optimistic calibration results. Under-fitting produces excessive bias in the outputs, whereas over-fitting produces excessive variance. Optimising the number of predictors will therefore reduce the tendency of calibrated MLR models to perform poorly when presented with new observations. Therefore, the MLR model development process involved consecutive addition of predictor variables starting with the highest correlated predictor. Each time a new predictor is added, cross correlation is carried out between predictors to screen out any correlated predictors from the equation. This is repeated until a reasonable number of predictors (usually 3 – 6) that produce high model efficiency is reached.

For each month, MLR model is fitted using observed monthly rainfall (evaporation) series as predictand and correlated large-scale monthly climatic predictors for the best-fit period. For the selected period, two thirds of the series will be used for calibration and one third for verification. For a shorter period like 1961-1979, verification by replacement will be used in which each the model is calibrated excluding one data point and verified by including the excluded data point while excluding one data point used during the calibration.

3.3.2.2.2 MLR model evaluation

Several criteria for evaluating performance of models currently exists.The two criteria are adopted for this study which are the Nash-Sutcliffe coefficient of efficiency (CE) and the index of volumetric fit (IVF). The CE is given by

$$CE = 1 - \frac{\sum (y_{obs} - y_{pred})^2}{\sum (y_{obs} - \bar{y}_{obs})^2} \quad (3.2)$$

where y_{obs} and y_{pred} are observed and predicted elements, $\bar{y}_{obs}$ is the average of the observed elements and *n* is the record length.

The IVF is given by

$$IVF = \frac{\sum_{1}^{n} (Q_e)_i}{\sum_{1}^{n} (Q_0)_i} \quad (3.3)$$

where Q_e and Q_o are estimated and observed predictand values in time (e.g. day, month) *i*.

The CE is appropriate for indicating model efficiency in reproducing the inherent variance (variability) in the predictand while IVF is appropriate for indicating the volumetric fit between observed and estimated series. The latter criterion is useful in climate modelling due to inherent weakness of existing GCMs in reproducing existing variability of most climatic variables.

3.3.3 Assessment of GCM capability

The assessment of capability of various GCMs to reproduce the current Pangani climate will be carried using developed MLR models and GCM simulation outputs for the same period used for model calibration (either 1961-2001, 1961-1979 or 1980-2001). The procedure will involve driving the MLR models by GCM predictors and assessing the performance by model efficiency criteria (IVF and/or CE). Those GCMs that reproduce well the current climate of Pangani will be selected for scenarios development.

3.3.4 Development of future rainfall and evaporation series

Since all future emission scenarios are likely to occur, the development of climate changes scenarios of rainfall and evaporation for catchments in the Pangani basin involved the use of ensemble GCM outputs computed as the averages of outputs from all GCMs which reproduce well the current climate.

The future GCM predictor series are used to drive developed MLR models to obtain future series of rainfall and evaporation. Since GCM predictions of absolute values are relatively poor, the averages for the 30-year periods (2010-2039, 2040-2069 and 2070-2099) are be computed and the changes with respect

to baseline 1961-1990 period established. The changes will then be used to construct the modified catchment rainfall and evaporation series for the three future periods.

In order to establish the wet and dry future climates of Pangani, variance is computed for each predicted series for the 2010-2039, 2040-2069 and 2070-2099 periods. The present day variance level (e.g. 1σ – one standard deviation, etc) that is related to wetness or dryness of the year is presumed to prevail in the future and is applied to modify the estimated future rainfall and evaporation series. This procedure will provide wet and dry rainfall series from which their 30-year averages are computed to establish the change with respect to baseline period. The changes are then used to construct the modified catchment rainfall and evaporation series for the three future periods for the wet and dry climate scenarios.

4 FUTURE RAINFALL AND EVAPORATION SERIES FOR PANGANI

4.1 INTRODUCTION

This section presents overall procedure of the establishment of statistical odwnscaling models, discusses corresponding results and provide modified series of rainfall and evaporation for anticipated future average, wetter and drier conditions in Pangani basin.

4.2 RAINFALL AND EVAPORATION DOWNSCALING

4.2.1 Selection of climatic predictors for rainfall

The modelling experience and literature provided useful information on the seasonality of climatic influences and potential predictor climatic variables for rainfall prediction in Pangani basin. However, most of documented work is related to seasonal rainfall amounts and extensively use SSTs and SOI although some have used atmospheric winds. The small spatial scale of this study is also an important distinction to past regional scale studies while the need to use those climatic variables which are direct output of GCM with low spatial variance is considered. All this indicated the need to precisely identify the rainfall-climatic variables relationships from the catchment scale perspective using monthly rainfall and evaporation series.

Correlation analysis was used in the preliminary analysis involving five variables, mean sea level pressure (MSLP), zonal (U) and meridional (V) winds and relative humidity to represent atmospheric moisture. Winds and humidity were considered at the surface, lower (850 hPa) and middle (500 hPa) tropospheric levels. The major criterion was the identification of moisture sources and the seasonality from humidity data and moisture transport by winds. This initial stage and model calibration and verification used NCEP/NCAR reanalyses. Although SST is currently utilised in most operational models, it was not considered in this study as it is only available for some GCMs (e.g. CSIRO Mark II, CCCMa CGCM2, Table 3.1).

The results indicated the tropical western Indian Ocean as the major source of moisture into Pangani and winds over Somali, coastal areas, thermocline dome and tropical southwestern Indian Ocean (East Madagascar and Mozambican Channel) advect seasonally this moisture into Pangani (Fig 4.1). The correlations further indicates a general mainly influence of austral (southern) winter (June-August) and Spring (September-November) and a moderate influence of austral summer (December-February). The East Madagascar (southwestern Indian Ocean) contributes moisture the earliest in July followed by the Mozambican Channel and thermocline dome in August-September before the coastal and

Somali basins in October (Fig 4.2). The coastal and Mozambican channel basins are the only basins with moisture predictors in November while Somali has in December and coastal and Mozambican channel in January. This pattern could be reflecting the surface ocean water recirculation in the region and the role of the deep thermocline in the modulation of ocean surface water temperatures.

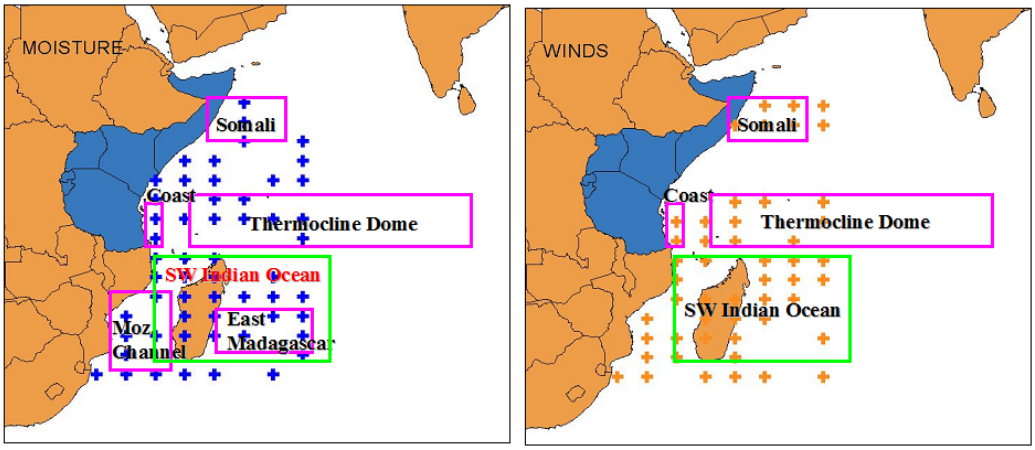

Fig 4.1: Sources of moisture for and moisture transporting winds into Pangani.

The highest correlations between rainfall and relative humidity were found in areas nearest to the coast and along the stretch extending southeast from the Tanzania coast to eastern Madagascar. On the other hand, negative and highest correlation between rainfall and winds were found in the Somali basin. Unlike moisture seasonality, different basins have seasonally varying influences on Pangani rainfall in relation to winds due to the monsoon changes. The northeast and southeast monsoon winds are related to influence of winds in almost the whole western Indian Ocean (Fig 4.2). The strongest influences of the Somali upwelling zone is experienced in September-October, thermocline dome in September-April, East Madagascar in November-April and Mozambican Channel in July-January).

4.2.2 Selection of climatic predictors for evaporation

Owing to the lack of time series of evaporation data during the time of execution of the study, it was not possible to carry out similar correlational analyses between observed evaporation series and influencing climatic variables such as winds, temperatures, etc. It is expected that future availability of such series will make this process possible.

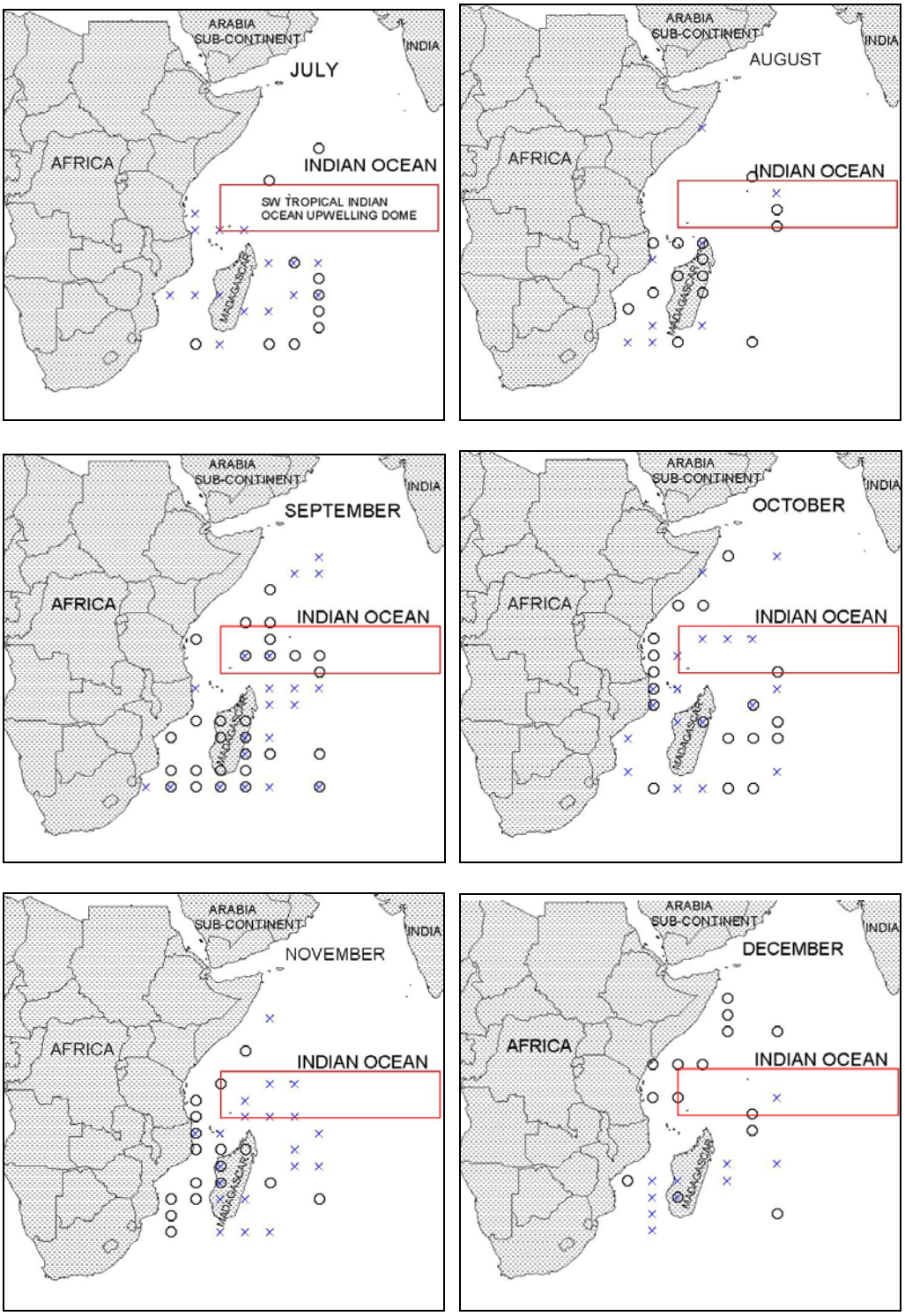

Fig 4.2: Location of atmospheric predictors: zonal winds (crosses) and 850hPa relative humidity (circles) in the Western Indian Ocean.

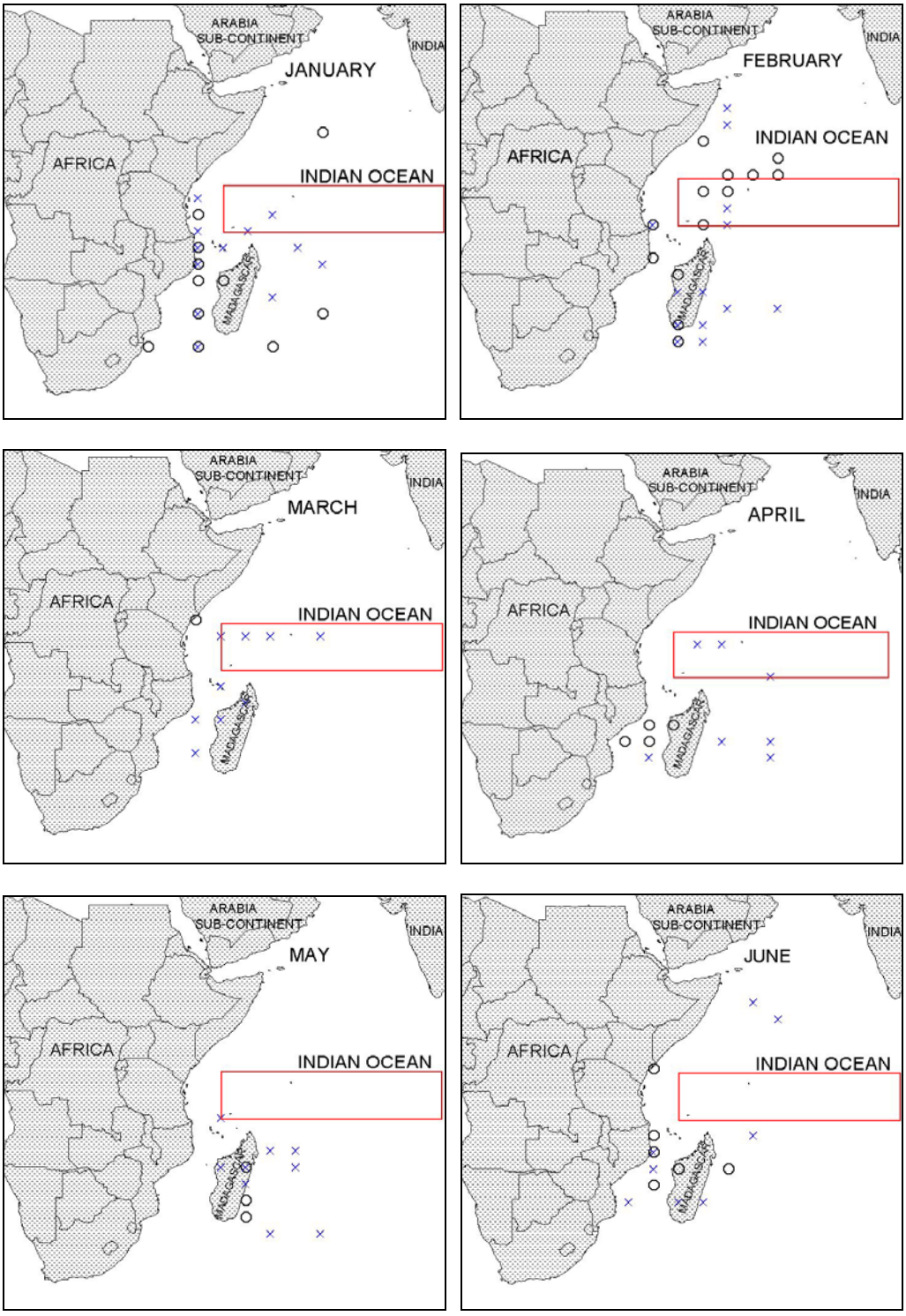

Fig 4.2: *Continued*.

4.2.3 Calibration and verification of rainfall models

Multiple Linear Regression (MLR) models were developed for the 1961-2001 period between catchment monthly rainfalls and NCEP/NCAR monthly reanalyses (climatic predictors) in selected gridboxes possessing high influences on rainfall variability in Pangani basin. The calibration and verification process involved the use of recent results (Richard *et al*., 2000; Valimba, 2005, Valimba and Mkhandi, 2007) of changing association between rainfall and climatic variables in the 1970s due to changes of rainfall (Valimba, 2005) and climatic variables (Trenberth, 1990, Kerr, 1992, Wang, 1995, Trenberth and Hoar, 1996, Tzarska *et al*., 1996;). The models were therefore developed for the whole 1961-2001 period and separately for 1961-1979 and 1980-2001. The model performance was evaluated using two criteria, the Nash-Sutcliff coefficiency of efficiency (CE or R^2) and the index of volumetric fit (IVF).

Results indicate either improvement or deterioration of CE in the recent 1980-2001 compared to the 1961-1979 period (e.g. Table 4.2) and that the low CE in the 1961-2001 period are contributed by the low efficiencies in either of the two sub-periods. The latter 1980-2001 period is considered relatively stationary and predominantly better CE suggest the suitability of this period for prediction purposes.

Table 4.2: Example of changing CE (%) for different periods in 1961-2001.

Catch	Period	Oct	Nov	Dec	Jan	Feb	Mar
1d14	1961-2001	32.8	34.4	46.3	30.6	49.5	22.8
	1961-1979	34.0	45.2	15.1	34.1	28.2	22.4
	1980-2001	33.1	28.0	60.5	27.5	70.8	22.8
1db2a	1961-2001	43.8	45.1	65.9	49.8	38.6	49.4
	1961-1979	23.8	59.9	42.8	26.5	23.6	61.7
	1980-2001	57.9	48.1	79.9	76.7	58.4	51.5
1dc1	1961-2001	33.0	56.7	67.0	51.8	63.8	47.2
	1961-1979	52.4	72.7	58.0	39.7	38.3	44.3
	1980-2001	31.9	40.9	80.4	73.3	80.2	68.9

Results for the 1980-2001 period (Table 4.3) indicated highly varying CE between different months and from one catchment to another. The prediction skills are moderate to high for monthly rainfalls during the dry June-September period and end of short rains (December) and transition period (January-February) (CE: 60 – 81%). Models have low performance during the core of the long rains in April suggesting that some other land processes may have significant contribution towards rainfall variability. Spatially, the model prediction skills are higher in the upper catchments in the basin and low in most catchments in the central, representing the main River Pangani and downstream Luengera sub-basin (Table 4.3).

Most existing GCMs have low skills to reproduce interannual variability of some climatic variables in certain regions and this has necessitated the use of 30-year averages in impact studies and assess model performance by IVF. Despite low CE for some months, the IVF for unadjusted model parameters were close to 1.0, ranging mostly between 0.9998 and 1.0005 (Table 4.4).

Table 4.3: Model efficiency criterion (CE) between observed catchment monthly rainfall in Pangani and observed climatic predictors for the 1980-2001 period. Moderate efficiencies are shown in blue.

Catch	Oct	Nov	Dec	Jan	Feb	Mar	Apr	May	Jun	Jul	Aug	Sep
1d10	37.6	17.9	68.3	26.3	35.8	20.3	8.4	33.7	43.1	**70.4**	37.4	63.1
1d14	33.1	28.0	60.5	27.5	**70.8**	22.8	43.1	39.5	35.6	63.7	**69.9**	**71.3**
1d17	36.0	19.0	*54.6*	25.4	*55.5*	17.9	*53.7*	39.4	42.1	*57.2*	65.2	41.9
1da1	*53.3*	26.8	*57.0*	49.7	46.2	11.8	42.8	29.9	33.0	*56.6*	14.7	22.6
1da3	30.6	*51.6*	39.8	38.4	62.4	42.1	38.4	33.4	41.5	*51.6*	49.0	*52.5*
1db17	46.6	45.5	*57.5*	67.8	*52.3*	*57.0*	42.7	44.9	45.3	44.7	63.6	*52.8*
1db18	*51.2*	25.3	62.6	64.2	39.9	*55.0*	63.3	*55.1*	61.3	*51.4*	*53.2*	**75.1**
1db19	43.8	*50.6*	*50.1*	35.5	*53.7*	*50.2*	*52.8*	61.1	*53.4*	44.8	65.3	48.3
1db2a	*57.9*	48.1	**79.9**	**76.7**	*58.4*	*51.5*	63.3	*55.1*	61.3	*51.4*	*53.2*	**75.1**
1dc11	39.5	27.0	**74.6**	**78.4**	60.3	*53.3*	11.9	65.2	46.5	68.2	*52.8*	48.4
1dc1	31.9	40.9	**80.4**	**73.3**	**80.2**	68.9	24.0	44.7	**77.0**	**70.9**	64.1	*57.3*
1dc2a	*51.2*	40.7	**78.6**	**76.8**	61.2	*57.3*	48.4	62.9	64.7	**71.8**	**77.9**	67.4
1dd1	*54.5*	32.2	**74.2**	44.8	*53.8*	63.3	33.8	44.1	**72.9**	*53.9*	46.0	*54.8*
1dd54	60.1	*53.5*	**79.0**	67.0	60.9	*59.1*	14.5	**79.0**	18.8	**72.0**	*57.8*	**75.6**
1dd55	63.4	*50.7*	**70.0**	*59.1*	**71.7**	67.0	38.3	**85.2**	27.7	59.8	**72.1**	64.3
Estuary	31.4	32.2	61.9	62.7	54.1	49.7	68.2	48.9	33.4	41.3	*51.8*	32.5

4.2.4 GCM prediction capability

4.2.4.1 Selection of suitable GCMs

A study on the suitability of 17 among the 22 coupled GCMs submitted for inclusion in the IPCC Fourth Assessment Report (Saji *et al*., 2007) to simulate the climate variability of the Indian Ocean indicated three main groups. The first includes GCMs which simulates relatively well the conditions in the Indian and Pacific Oceans with slight different location of the tropical thermocline dome. They include the China's IAP's FGOALS1 g1.0 model, French CNRM CM3 and American GFDL CM2.1 and NCAR PCM. The second group includes such models which simulate slightly less accurately the variable values in the Indian Ocean but more accurately the location of the thermocline dome and related features. They include the British UKMO HadCM3. The third group includes those models which less accurately and sometimes erroneously simulate the major conditions in the two oceans and includes the Canadian CCCMa CGCM3.1 and American GISS-AOM. Only two representative GCMs will therefore be selected from the first two groups for use in this study.

The HadCM3 is selected from the second group as it is the only candidate GCM in the group. From the first group, a comparison of correlation patterns between Nino-3 and Indian Ocean SST anomalies (Saji *et al*., 2006) indicated that GFDL CM2.1 displays similar pattern to that shown by observed data. This GCM further simulates better the tropical western Indian Ocean thermocline dome than other GCMs in the group and it was therefore selected for the downscaling.

4.2.4.2 Assessment of efficiency of selected GCMs

Despite good CE for some monthly rainfall in certain catchments, downscaled monthly rainfall using HadCM3 and GFDL CM2.1 climatic predictors for the 1980-2001 period varied between the two GCMs. Whilst GFDL CM2.1 gave predominantly positive and sometimes good IVF, a number of negative and poor

IVF were obtained when HadCM3 downscaled rainfalls were compared to observed (Table 4.4). Considering IVF within 25% of unit (0.75 – 1.25), only a few models have relatively good IVF (Table 4.3).

Table 4.4: IVF between observed catchment monthly rainfall in Pangani and NCEP/NCAR, HADCM3 and GFDL CGCM2.1 estimated monthly rainfall for the 1980-2001 period. Negative IVF are in italics.

Station	Clim pred	Jan	Feb	Mar	Apr	May	Jun	Jul	Aug	Sep	Oct	Nov	Dec
	NCEP/NCAR	0.9504	1.0000	1.0000	1.0000	1.0000	0.9996	1.0005	1.0002	1.2912	1.0000	1.0000	1.0000
	GFDL 2.1	1.6905	1.0480	1.1691	0.9169	1.1990	2.4842	2.4851	1.3158	0.4114	0.9913	1.1050	1.1392
1d10	HADCM3	0.1113	*-0.6586*	0.9372	1.6010	3.0261	1.5218	1.5268	*-1.2955*	*-0.0956*	*-0.1769*	0.6155	2.0355
	NCEP/NCAR	1.0000	0.9999	1.0000	1.0000	1.0000	0.9993	1.0002	0.9999	0.9999	1.0001	1.0001	1.0001
	GFDL 2.1	1.5555	2.6829	1.1760	0.9542	0.8132	1.8500	1.8509	0.8407	2.6246	1.4559	1.4346	0.0759
1d14	HADCM3	*-0.3383*	*-4.4202*	0.9422	*-0.8304*	1.1613	0.6072	0.6122	*-5.5920*	8.0426	1.0387	0.6655	2.2829
	NCEP/NCAR	1.0000	1.0000	1.0000	1.0000	1.0000	0.9992	1.0001	0.9999	0.9999	1.0000	1.0001	1.0000
	GFDL 2.1	1.8100	3.6168	1.1781	0.9745	1.0065	1.7952	1.7961	0.9695	1.5580	1.2998	1.3174	0.9067
1d17	HADCM3	0.0816	*-6.0718*	1.2365	*-0.9103*	0.7800	0.0817	0.0867	*-2.5568*	1.3559	1.0519	0.7452	2.0447
	NCEP/NCAR	1.0000	1.0000	1.0000	1.0000	1.0000	0.9992	1.0001	0.9999	1.0002	1.0000	1.0000	0.9999
	GFDL 2.1	*-0.1368*	1.1416	1.0798	0.9218	0.7285	2.2575	2.2584	*-0.0571*	1.6367	2.7474	1.2745	1.0658
1da1	HADCM3	1.5234	*-1.6346*	0.9881	*-0.4395*	1.2058	2.2534	2.2584	*-0.0571*	1.0681	0.0747	0.7315	1.9620
	NCEP/NCAR	1.0000	1.0001	1.0000	1.0000	1.0000	0.9991	1.0000	1.0001	0.9969	1.0000	1.0000	1.0000
	GFDL 2.1	0.7644	1.3702	0.8845	*-0.0705*	1.1675	1.8780	1.8789	0.5187	2.7686	1.1287	0.3133	0.5183
1da3	HADCM3	0.1557	*-2.0634*	0.7963	*-0.0705*	0.7744	0.9529	0.9579	2.5522	1.1123	1.1404	1.8150	0.8743
	NCEP/NCAR	1.0000	0.9999	1.0000	1.0000	1.0000	0.9989	0.9998	1.0001	0.9997	1.0000	1.0000	1.0000
	GFDL 2.1	*-0.1120*	2.5882	1.7775	1.2973	1.2086	0.3770	0.3779	2.0413	2.1392	0.8050	0.4370	1.4114
1db17	HADCM3	1.5121	*-2.5058*	0.6430	*-1.7581*	1.1465	3.0749	3.0799	0.0719	2.3286	3.1408	1.6931	1.6438
	NCEP/NCAR	1.0000	1.0000	1.0000	1.0000	1.0000	1.0002	1.0000	1.0124	0.9993	1.0000	1.0000	1.0000
	GFDL 2.1	*-0.0030*	1.8420	2.3360	0.6043	0.8679	2.2986	2.4986	1.2191	2.9363	0.3049	0.6304	1.1514
1db18	HADCM3	1.3696	*-2.3573*	*-0.2451*	1.6343	0.0823	*-1.9722*	0.5397	1.4851	1.1114	1.6567	1.3714	2.0380
	NCEP/NCAR	1.0000	1.0001	1.0000	1.0000	1.0001	0.9989	0.9998	0.9999	0.9998	0.9999	1.0000	1.0000
	GFDL 2.1	0.7612	2.4867	1.7121	0.9993	0.8058	1.3428	1.3437	1.5553	2.3946	0.7829	0.2883	1.4585
1db19	HADCM3	0.1442	*-2.4007*	0.6523	1.5233	1.2976	2.6121	2.6171	*-0.6413*	1.6061	2.9474	1.8735	*-1.5088*
	NCEP/NCAR	1.0000	1.0000	1.0000	1.0000	1.0000	1.0002	1.0000	1.0124	0.9993	0.9999	1.0000	1.0000
	GFDL 2.1	0.5146	1.6400	1.7226	0.5687	0.3589	2.2986	2.4986	1.2191	2.9363	0.7016	0.4790	1.0051
1db2a	HADCM3	1.5998	*-1.8146*	0.1695	2.1906	1.5583	*-1.9722*	0.5397	1.4851	1.1114	1.8857	1.6892	3.6401
	NCEP/NCAR	1.0000	1.0001	0.9999	1.0000	1.0000	1.0000	0.9998	0.9997	1.0002	1.0000	0.9998	0.9900
	GFDL 2.1	0.7861	1.2979	1.2437	0.9488	0.6115	1.2131	2.0637	*-0.2182*	1.5230	0.8174	0.8037	0.6745
1dc11	HADCM3	0.7262	*-1.7016*	0.1227	1.2608	1.3529	0.8671	0.8851	2.5741	0.7579	0.1077	1.4096	1.0808
	NCEP/NCAR	1.0000	1.0001	1.0001	1.0000	1.0000	1.0000	0.9996	0.9998	1.0005	1.0001	1.0000	1.0000
	GFDL 2.1	0.6179	0.8677	1.9461	0.8156	1.1517	1.0217	1.4029	2.2816	1.9327	0.3919	1.1314	0.7477
1dc1	HADCM3	0.3777	*-2.2453*	0.4291	3.4870	0.8229	2.4021	2.6044	*-0.2959*	1.9199	1.2432	0.5187	0.4519
	NCEP/NCAR	1.0000	0.9999	1.0000	1.0000	1.0001	1.0003	1.0002	1.0001	0.9999	1.0000	1.0000	1.0000
	GFDL 2.1	*-0.3463*	1.0794	1.7252	0.9947	0.5000	1.6389	2.9646	1.2333	1.9446	*-0.4060*	0.7903	0.7347
1dc2a	HADCM3	0.9922	*-1.6606*	0.0450	1.4956	0.3839	4.5391	1.4467	0.8275	1.9031	*-2.0958*	1.5057	*-0.6328*
	NCEP/NCAR	0.9999	0.9999	1.0000	1.0000	0.9996	1.0000	1.0000	0.9999	1.0002	1.0001	1.0001	0.9999
	GFDL 2.1	1.1405	2.3539	1.5658	1.0181	0.8472	2.3464	1.0756	1.3683	0.6305	1.1727	0.7409	0.7402
1dd1	HADCM3	*-0.6805*	*-4.0083*	0.6699	2.0480	0.9830	2.0484	3.3470	0.9126	1.7850	2.7883	1.4050	0.1094
	NCEP/NCAR	1.0000	0.9999	1.0000	1.0000	1.0000	0.9998	1.0004	1.0004	1.0004	1.0001	1.0000	0.9999
	GFDL 2.1	0.5957	1.5879	0.5491	0.8453	0.1286	0.6261	0.9864	0.6422	1.0977	0.3533	0.7905	0.0683
1dd54	HADCM3	0.3266	*-0.8510*	*-0.2713*	1.4300	1.2662	0.6839	0.8704	1.3069	4.1332	*-0.3546*	0.4431	0.9399
	NCEP/NCAR	1.0001	1.0000	1.0000	1.0000	1.0000	1.0000	1.0010	1.0004	1.0006	0.9999	1.0001	0.9999
	GFDL 2.1	*-0.0653*	2.2112	0.5944	0.8801	*-0.4897*	0.4971	*-0.3562*	2.1642	2.7056	0.3155	0.6968	0.5872
1dd55	HADCM3	1.1051	*-2.8006*	*-0.2235*	1.9636	0.7689	2.5253	3.6142	*-1.2106*	3.4004	1.6914	0.5370	0.6978
	NCEP/NCAR	1.0001	1.0001	1.0001	1.0000	1.0000	1.0000	1.0000	1.0001	1.0000	1.0000	1.0000	1.0001
	GFDL 2.1	2.2483	1.7378	0.8954	0.9357	1.2295	0.8333	1.0936	1.7888	2.2240	0.5428	0.6739	1.6915
Estuary	HADCM3	*-0.0125*	*-4.4580*	1.4396	1.4566	*-0.0006*	0.7735	1.3639	*-0.4731*	1.7425	1.7913	0.7151	3.0408

Correlation analysis between NCEP/NCAR reanalyses and HadCM3 and GFDL CM2.1 predictor variables for 1961-2001 and 1980-2001 periods indicated predominance of low correlations with few moderate positive and negative

correlations. This is anticipated due to low GCM skills to reproduce interannual variance inherent in the observed series. The predominant positive correlations for HadCM3 prevail between the climatic variables in the coastal and equatorial central Indian Ocean basins (from the east African coast to west of 60°E, between equator and 12°S). The predominant negative correlations are shown by climatic variables in the southwest Indian Ocean (SWIO) basin extending from the southern African coast to west of 60°E (12°S – 27°S). This suggests a low HadCM3 skill to reproduce low-level climatic signals over the SWIO and moderate skills that reproduce interannual variability of climatic variables over equatorial Indian Ocean (e.g. Fig 4.2).

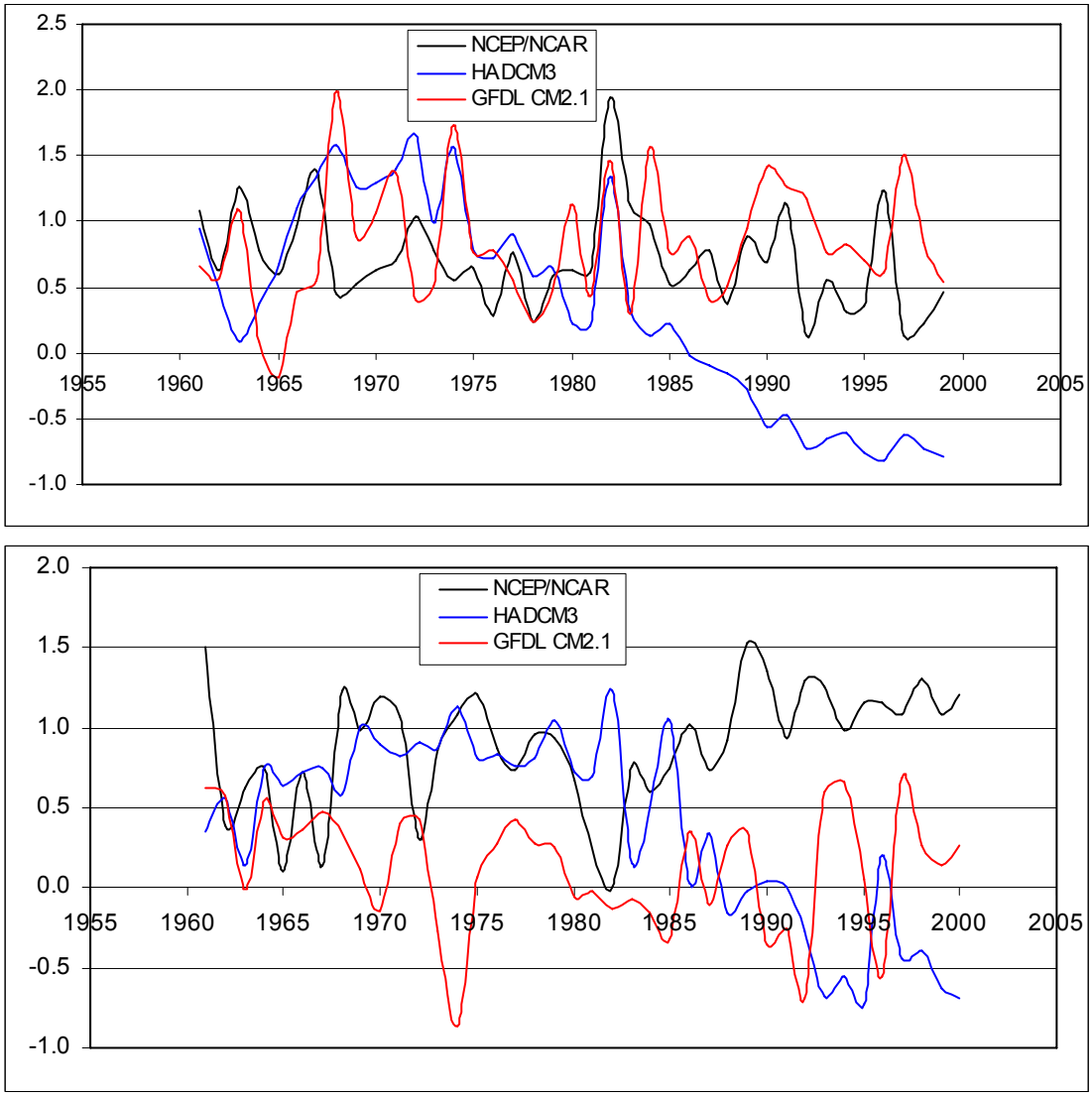

Fig 4.2: Comparison of NCEP/NCAR, HadCM3 and GFDL CM2.1 a) October and b) December zonal winds at gridboxes in Southwest Indian Ocean.

However, GFDL CM2.1 shows comparable pattern of variability and magnitude of anomalies with that of NCEP/NCAR variables. It was therefore, considered appropriate to introduce some adjustment of calibrated MLR model parameters

when using GFDL CM2.1 variables to bring IVF close to 1.0000. The adjustments significantly improved IVF between observed series and GFDL CM2.1 downscaled rainfall series (Table 4.5). The modifications, however, decreased CE slightly to significantly depending on the effected parameter changes while in a few cases of inappropriateness of changes were encountered for February rainfall at 1d17, 1db17, 1db18 and 1db19. The models were therefore considered adequate and used to estimate future monthly rainfalls in Pangani.

Table 4.5: IVF between observed catchment monthly rainfall in Pangani and NCEP/NCAR and GFDL CGCM2.1 estimated monthly rainfall for the 1980-2001 period for modified MLR model parameters.

Station	Clim pred	Jan	Feb	Mar	Apr	May	Jun	Jul	Aug	Sep	Oct	Nov	Dec
1d10	NCEP/NCAR	0.7727	1.0000	0.9997	1.0385	0.9556	**0.8657**	0.8834	1.0065	1.0446	1.0000	0.9917	1.0203
	GFDL 2.1	1.2537	1.0480	1.0669	0.9811	1.1645	**1.0810**	1.1030	1.0226	1.0135	0.9913	1.0778	1.0562
1d14	NCEP/NCAR	0.8561	0.9891	0.9830	1.0366	1.0587	**0.9767**	0.9966	1.0767	0.9999	1.0227	0.9962	0.8225
	GFDL 2.1	1.2728	1.1503	1.0352	0.9931	1.0014	**1.0501**	1.0715	0.9995	2.6246	0.9948	1.0552	0.8009
1d17	NCEP/NCAR	0.7777	1.0000	1.0000	1.0199	1.0000	**0.9829**	1.0030	1.0064	1.0869	1.0053	1.0108	1.0048
	GFDL 2.1	1.2637	3.6168	1.1781	0.9955	1.0065	**0.9838**	1.0039	1.0028	1.0811	1.0248	1.0502	0.9965
1da1	NCEP/NCAR	1.1709	1.0000	1.0000	1.0665	1.0834	**0.9940**	1.0143	1.0008	1.0928	1.0113	0.9611	0.9999
	GFDL 2.1	0.7731	1.1416	1.0798	0.9922	0.9960	**1.0975**	1.1199	1.3450	1.0996	0.9903	1.0963	1.0658
1da3	NCEP/NCAR	1.1137	0.9915	1.0138	1.0000	0.9997	**0.9627**	0.9823	1.0067	0.9969	1.0177	1.0447	1.0667
	GFDL 2.1	0.8309	1.0310	0.9990	1.1402	1.0659	**1.0336**	1.0547	1.0173	2.7686	1.0022	0.9760	1.0558
1db17	NCEP/NCAR	1.1904	0.9999	1.0138	0.9151	1.0009	**1.0016**	1.0221	1.0972	1.0095	1.0109	1.0840	1.0096
	GFDL 2.1	0.9013	2.5882	0.9918	1.0899	1.0737	**0.9715**	0.9913	0.9861	0.9951	1.0565	0.9994	1.0424
1db18	NCEP/NCAR	1.1125	0.9011	0.5526	1.0754	1.0058	1.0015	0.9902	1.0068	0.9195	0.9972	1.0080	1.0282
	GFDL 2.1	0.9153	1.5709	1.2421	0.9944	0.9959	1.0625	1.0998	1.0652	1.9104	1.0172	1.0003	1.0363
1db19	NCEP/NCAR	1.1151	1.0001	1.0115	1.0000	1.0776	**0.9890**	1.0092	0.8191	0.9998	1.0227	1.0117	0.9784
	GFDL 2.1	0.8286	2.4867	1.0158	0.9993	0.9749	**1.0130**	1.0337	1.0919	2.3946	1.0372	0.9405	1.0961
1db2a	NCEP/NCAR	1.0280	0.9612	0.8802	1.0704	1.0256	1.0015	0.9902	1.0068	0.9195	1.0566	1.0732	1.0000
	GFDL 2.1	0.9951	1.3265	1.2102	1.0156	1.0052	1.0625	1.0998	1.0652	1.9104	1.0007	0.9753	1.0051
1dc11	NCEP/NCAR	1.0108	0.9944	1.0171	1.0299	1.0997	0.9988	1.0164	1.1958	1.0040	0.9935	1.0575	0.9982
	GFDL 2.1	1.0099	1.0740	0.9995	0.9985	0.9902	1.0241	0.9984	0.9493	1.0472	0.9915	0.9928	1.0380
1dc1	NCEP/NCAR	1.0768	1.0410	1.0142	1.0936	0.9928	1.0000	1.0093	0.9049	1.0014	0.8197	0.9826	1.0005
	GFDL 2.1	1.0015	1.0015	1.0643	0.9067	1.0202	1.0217	1.0410	1.1947	1.0433	0.6372	1.0746	0.9879
1dc2a	NCEP/NCAR	1.1951	0.9999	1.0024	1.0000	1.0955	0.9328	1.0002	1.0010	0.9418	1.0510	1.0060	1.0397
	GFDL 2.1	0.9256	1.0794	1.0820	0.9947	0.9085	1.1800	1.1738	1.0377	1.1091	1.0029	1.0440	1.0086
1dd1	NCEP/NCAR	0.9822	1.0003	1.0097	1.0000	1.0164	1.0000	1.0000	1.0062	1.0093	1.0003	1.0976	1.0888
	GFDL 2.1	1.0299	1.0256	1.0004	1.0181	1.0020	0.9998	1.0756	1.0007	1.0038	1.0413	1.0008	1.0171
1dd54	NCEP/NCAR	1.1361	0.6223	0.9499	1.0792	1.1438	1.1873	1.0004	1.1542	1.0004	1.0898	1.1228	0.9179
	GFDL 2.1	1.0011	0.9948	1.0595	0.9969	0.9511	1.0134	0.9864	0.9010	1.0977	1.0029	0.9878	0.9835
1dd55	NCEP/NCAR	1.1299	0.8101	1.0406	1.0799	1.0194	1.2232	1.1934	0.8250	1.0006	1.0596	1.0751	1.0415
	GFDL 2.1	0.9035	1.4963	0.9635	0.9739	0.9841	0.8656	0.8115	1.2081	2.7056	1.0200	0.9920	0.9990
Estuary	NCEP/NCAR	0.8024	0.9334	1.0681	1.0486	0.9998	1.1093	1.0000	0.9122	0.9108	0.9650	1.0515	1.0163
	GFDL 2.1	1.2780	1.1758	1.0049	1.0006	1.0067	0.9751	1.0936	1.0148	1.1970	0.9193	1.0061	1.0030

4.3 MODIFIED RAINFALL AND EVAPORATION SERIES

4.3.1 Modified rainfall series

4.3.1.1 Rainfall series for average conditions

Successfully calibrated and verified rainfall-climatic variables MLR models were run using GCM derived climatic predictors to provide time series of monthly rainfalls for the periods 2010-2039 (2020s), 2040-2069 (2050s) and 2070-2099 (2080s). The series were used to compute the 30-years averages to represent

the average rainfall conditions in the short term (2020s), medium term (2050s) and long term (2080s) respectively. The predicted averages were then compared to the 1961-1990 average of the observed monthly rainfalls and departure from the 1961-1990 average was expressed as percentages of the 1961-1990 averages. These changes were used to establish rainfall series for 2020s, 2050s and 2080s. The observed monthly rainfall series (Beuster *et al*., 2006) are therefore multiplied by a factor computed as (1+ change) to obtain future series. For example, a rainfall decline of 27% means the rainfall series is modified through multiplication by a factor of 1 – 27/100 = 0.73. This procedure was used to establish new modified monthly rainfall series, which are provided separately as MS Excel worksheets as supporting document to this draft.

Results indicate varying future rainfall conditions in different months. They indicate predominant decrease of rainfall in the October-January affecting significantly the short rains occurring between late October and mid December/early January (Table 4.6, Fig 4.3). The results indicate, for example, a decline of 10% - 100% of October rainfall suggesting its disappearance in some catchments. Despite this latter observation, which may be attributed by the low reliability of GCM predictor variables and model performance, the general trend is towards declining short rains. This is a general anticipated response of increasing global air and ocean temperatures that translate into reduction of orographic rainfall (which is predominant during the short rains) and an increase of convective rainfall. The results further indicated slight changes of the long rains usually received in March-May period. The changes correspond to slight increase of April and/or May monthly rainfall (Table 4.6).

4.3.1.2 Correction for future rainfall scenarios

The rainfall scenarios resulting from direct use of calibrated MLR models (Table 4.6) are somehow unrealistic for some months in some catchments. This is illustrated by a complete disappearance (100% decrease) of October rainfall in the Kikuletwa catchment (1DD1) while a decrease of 46% and 44% is predicted by the middle and end of the 21st Century in the largest contributing catchment of 1DD54. Similar monthly rainfall scenarios are predicted in the adjacent eastern catchment of River Ruvu where generally a decrease of 40-49% of October rainfall is predicted at the contributing catchment of 1DC11 to the outlet at 1DC1 despite a predicted increase in another contributing catchment of 1DC2A (Table 4.6).

It was therefore necessary to introduce corrections to model predictions to provide spatially uniformity. The corrections were mainly done in the following two ways to estimate the change (%) for the catchments with unrealistic future predictions:

i) Spatial interpolation of percentage changes
ii) Estimation of percentage changes in nested catchments using changes in contributing catchments

Contours were used in the spatial interpolation process in which unrealistic predicted percentage changes were excluded during the interpolation. The 100% decrease of October rainfall at 1DD1, for example, was excluded during the interpolation analysis and contours within the catchment were averaged to estimate the percentage change in the catchment. For nested catchments like 1DC1, percentage changes were also estimated from changes in contributing

sub-catchments like 1DC11 and 1DC2A, which make the grand catchment. The estimation process involved:

i) establishment of area-weighted factors as fraction of total nested catchment area occupied by the sub-catchment
ii) establishment of sub-catchments percentage changes as a cumulative sum of weighted sub-catchment changes (factor x percent change)

Table 4.6: Simulated changes (%) of monthly rainfall in Pangani. Decreases are yellow filled, increases are light blue filled.

				Short Rains			Intermediate		Long Rains			Dry Season			
Sub-basin		Station	Period	Oct	Nov	Dec	Jan	Feb	Mar	Apr	May	Jun	Jul	Aug	Sep
KIKULETWA	Upper		2020s	-66.4	-1.8	7.2	-3.3	44.1	6.7	-1.8	-0.2	-8.9	-27.6	88.7	132.5
			2050s	**-100.0**	-13.2	1.1	-19.5	43.9	-14.7	0.8	-2.3	-30.2	-12.8	91.9	159.3
		1dd55	2080s	**-100.0**	-45.8	-8.0	-33.5	35.1	-4.8	-2.4	-0.4	-36.9	2.5	75.1	168.7
	Lower		2020s	11.8	-11.6	16.5	2.6	5.4	18.2	0.8	-20.5	9.2	-5.9	-16.1	7.2
			2050s	-46.0	-25.1	4.5	-65.1	-10.3	2.7	3.3	-14.8	24.3	13.0	-65.8	-30.5
		1dd54	2080s	-44.2	-63.7	8.0	-90.9	13.6	16.4	-3.2	-16.9	10.8	-14.4	**-100.0**	-10.3
			2020s	**-100.0**	-79.7	4.0	1.2	67.8	-23.6	4.9	1.6	1.6	-27.7	13.8	-11.7
			2050s	**-100.0**	**-100.0**	-10.1	-46.8	154.3	-18.5	10.7	-6.4	73.7	-51.8	19.4	32.6
		1dd1	2080s	**-100.0**	**-100.0**	-19.0	-79.2	**265.2**	29.4	9.6	-11.1	6.7	-60.1	21.3	-39.3
RUVU	Upper		2020s	-40.2	-37.4	9.8	-30.4	6.5	-6.7	-2.3	0.0	5.4	-3.3	-1.1	-0.3
			2050s	-43.0	-61.2	-10.5	**-100.0**	-70.0	11.1	3.6	11.7	11.9	22.9	-2.2	-14.8
		1dc11	2080s	-77.3	-99.7	-21.8	**-100.0**	-59.4	34.0	4.1	3.5	11.4	-2.4	-0.5	-14.5
	Lower		2020s	42.5	-1.8	20.6	-19.2	39.8	11.5	0.8	15.2	3.5	24.8	10.3	24.3
			2050s	45.5	-3.1	3.7	**-100.0**	-67.6	8.2	7.5	25.0	10.9	36.0	-3.7	-69.7
		1dc2a	2080s	**144.0**	-4.2	13.0	**-100.0**	-41.4	0.8	8.4	33.5	4.7	59.8	-51.8	**-100.0**
			2020s	-40.5	-13.5	9.9	-46.9	67.4	-9.0	-3.0	70.8	-32.5	0.6	10.1	38.9
			2050s	-45.3	-21.2	-3.8	-71.9	43.6	-45.2	-2.2	72.2	-42.6	0.8	15.2	15.2
		1dc1	2080s	-48.6	-35.8	2.8	**-100.0**	107.1	-36.0	1.1	78.0	-43.5	-18.8	13.8	-15.7
PANGANI MA	Upper		2020s	-70.3	-3.3	-8.3	0.6	49.3	2.9	-8.9	8.9	13.5	68.7	20.7	26.7
			2050s	-97.1	-18.5	-17.8	-21.1	13.4	6.4	-4.1	16.7	17.0	40.5	0.5	14.4
		1d10	2080s	**-100.0**	-40.3	-19.6	-55.9	-6.8	7.3	-2.0	5.1	21.0	71.0	-13.6	13.8
	Middle		2020s	-32.5	9.6	-20.6	25.5	11.1	-1.1	7.0	-12.7	9.5	7.9	7.8	**115.6**
			2050s	-37.0	2.3	-21.2	48.0	11.1	-5.3	-0.7	-6.4	-1.6	32.6	72.2	**166.1**
		1d14	2080s	-51.3	-15.2	-21.5	63.8	9.3	-11.4	6.2	-2.7	1.5	-14.9	74.4	**192.5**
	Lower		2020s	-23.0	8.7	-10.8	1.4	**260.1**	13.3	5.7	-4.6	5.4	6.9	25.8	59.2
			2050s	-25.6	2.2	-18.0	-20.6	**263.4**	2.8	6.9	10.6	-20.2	19.0	45.2	**370.6**
		1d17	2080s	-36.7	-13.0	-19.7	-55.7	**254.3**	-18.9	17.1	37.4	-18.0	-37.8	48.4	**507.6**
MKOMAZI	Upper		2020s	-89.5	-48.9	-11.5	-33.3	55.6	25.7	-9.6	-11.7	64.3	15.4	-1.0	14.1
		1db2a/1	2050s	**-100.0**	-69.5	-21.9	61.1	54.1	14.4	1.4	-9.1	72.6	22.0	-19.8	-12.3
		db18	2080s	**-100.0**	**-100.0**	-24.1	-22.5	51.1	26.8	-1.3	-16.6	**186.4**	18.7	-20.1	-9.5
	Lower		2020s	-20.5	-7.2	8.1	8.6	**139.9**	14.2	-5.8	-7.1	19.6	4.7	-11.7	119.9
			2050s	11.0	-10.2	6.5	-15.1	**159.6**	7.0	2.0	-11.4	30.0	9.1	-20.4	67.6
		1db19	2080s	36.2	-14.0	3.7	-31.3	**166.9**	-14.1	-14.7	-0.1	71.8	7.2	-37.2	61.2
			2020s	-22.6	-86.0	-28.6	-8.8	**147.8**	20.3	8.6	-1.0	-1.4	-16.9	-8.7	102.7
			2050s	16.1	**-100.0**	-10.6	-51.3	**172.5**	15.1	7.0	-11.7	-16.7	-15.4	-24.4	34.9
		1db17	2080s	47.0	**-100.0**	-18.0	-53.7	**183.0**	-6.9	5.4	-6.8	-9.7	-10.7	-38.3	64.7
LUENGERA	Upper		2020s	-12.5	-3.4	8.0	8.5	17.1	-2.6	14.0	5.1	21.8	11.2	1.3	**194.3**
			2050s	-23.2	-6.5	12.1	-14.9	41.0	-39.3	12.1	4.5	33.4	-6.9	35.4	**212.3**
		1da3	2080s	-24.8	-10.8	26.2	-30.8	49.0	-36.2	6.5	6.6	79.7	-12.1	6.3	**228.5**
	Lower		2020s	-20.7	-5.4	-4.2	-21.3	29.0	-2.2	3.0	-3.5	15.3	2.9	-47.8	-29.1
			2050s	-29.0	-24.5	-11.5	-79.7	2.0	-9.1	4.9	-3.0	23.4	9.8	-27.3	-84.3
		1da1	2080s	-83.8	-53.7	-12.3	-83.0	12.1	-24.2	14.6	-2.2	55.8	5.1	6.1	-93.6
ESTUARY			2020s	-10.4	-3.4	-31.4	-30.4	11.7	-6.1	-10.0	4.0	10.6	18.1	-14.6	-26.3
			2050s	-11.3	-33.5	-38.3	101.5	11.6	-12.3	-7.3	20.5	-23.7	6.4	-22.6	-77.7
		Estuary	2080s	-12.6	-47.5	-88.3	-31.4	8.9	-60.0	-18.8	49.1	-26.2	-4.2	-47.9	-64.7

Estimated percentage changes from interpolated changes were used to refine estimates from area-weighted changes for nested catchments and the overall

results of this correction process are provided in Table 4.7. The corrections have improved the developed future rainfall scenarios in most catchments.

Table 4.7: Corrected simulated changes (%) of monthly rainfall in Pangani. Decreases are yellow filled, increases are light blue filled.

Sub-basin		Station	Period	Short Rains			Intermediate		Long Rains			Dry Season			
				Oct	Nov	Dec	Jan	Feb	Mar	Apr	May	Jun	Jul	Aug	Sep
KIKULETWA	Upper		2020s	-66.4	-1.8	7.2	-3.3	44.1	6.7	-1.8	-0.2	-8.9	-27.6	88.7	132.5
			2050s	-100.0	-13.2	1.1	-19.5	43.9	-14.7	0.8	-2.3	-30.2	-12.8	91.9	159.3
		1dd55	2080s	-100.0	-45.8	-8.0	-33.5	35.1	-4.8	-2.4	-0.4	-36.9	2.5	75.1	168.7
	Lower		2020s	11.8	-11.6	16.5	2.6	5.4	18.2	0.8	-20.5	9.2	-5.9	-16.1	7.2
			2050s	-46.0	-25.1	4.5	-65.1	-10.3	2.7	3.3	-14.8	24.3	13.0	-65.8	-30.5
		1dd54	2080s	-44.2	-63.7	8.0	-90.9	13.6	16.4	-3.2	-16.9	10.8	-14.4	-100.0	-10.3
			2020s	-3.8	-9.6	14.6	1.2	13.1	-23.6	4.9	1.6	5.6	-27.7	13.8	-11.7
			2050s	-56.8	-22.7	3.8	-46.8	0.5	-18.5	10.7	-6.4	13.4	-51.8	19.4	32.6
		1dd1	2080s	-55.4	-60.1	4.8	-79.2	17.8	29.4	9.6	-11.1	1.3	-60.1	21.3	-39.3
RUVU	Upper		2020s	-40.2	-37.4	9.8	-30.4	6.5	-6.7	-2.3	0.0	5.4	-3.3	-1.1	-0.3
			2050s	-43.0	-61.2	-10.5	-100.0	-70.0	11.1	3.6	11.7	11.9	22.9	-2.2	-14.8
		1dc11	2080s	-77.3	-99.7	-21.8	-100.0	-59.4	34.0	4.1	3.5	11.4	-2.4	-0.5	-14.5
	Lower		2020s	-30.5	-4.2	20.6	-19.2	39.8	11.5	0.8	15.2	3.5	24.8	10.3	39.0
			2050s	-34.6	-5.9	3.7	-100.0	-67.6	8.2	7.5	25.0	10.9	36.0	-3.7	18.9
		1dc2a	2080s	-29.3	-10.9	13.0	-100.0	-41.4	0.8	8.4	33.5	4.7	59.8	-51.8	-12.1
			2020s	-40.5	-13.5	9.6	-46.9	31.5	-9.0	-3.0	11.4	-32.5	0.6	10.1	38.9
			2050s	-45.3	-21.2	-3.8	-71.9	-68.2	-45.2	-2.2	21.7	-42.6	0.8	15.2	15.2
		1dc1	2080s	-48.6	-35.8	2.8	-100.0	-45.6	-36.0	1.1	26.0	-43.5	-18.8	13.8	-15.7
PANGANI MAIN	Upper		2020s	-42.0	-3.3	-8.3	0.6	49.3	2.9	-8.9	8.9	13.5	68.7	20.7	26.7
			2050s	-48.4	-18.5	-17.8	-21.1	13.4	6.4	-4.1	16.7	17.0	40.5	0.5	14.4
		1d10	2080s	-65.9	-40.3	-19.6	-55.9	-6.8	7.3	-2.0	5.1	21.0	71.0	-13.6	13.8
	Middle		2020s	-32.5	9.6	-20.6	1.0	11.1	-1.1	7.0	-12.7	9.5	7.9	23.3	43.0
			2050s	-37.0	2.3	-21.2	-20.9	11.1	-5.3	-0.7	-6.4	-1.6	32.6	22.9	24.4
		1d14	2080s	-51.3	-15.2	-21.5	-55.8	9.3	-11.4	6.2	-2.7	1.5	-14.9	17.4	109.3
	Lower		2020s	-23.0	8.7	-10.8	1.4	16.6	13.3	5.7	-4.6	5.4	6.9	25.8	59.2
			2050s	-25.6	2.2	-18.0	-20.6	7.4	2.8	6.9	10.6	-20.2	19.0	45.2	34.4
		1d17	2080s	-36.7	-13.0	-19.7	-55.7	63.3	-18.9	17.1	37.4	-18.0	-37.8	48.4	**204.9**
MKOMAZI	Upper		2020s	-29.6	-6.0	-20.5	-47.2	35.3	16.9	-6.2	16.7	64.3	15.4	-1.0	14.1
		1db2a/1	2050s	-83.6	-29.9	-10.0	8.6	14.8	7.9	6.0	5.9	72.6	22.0	-19.8	-12.3
		db18	2080s	-95.1	-61.3	-31.1	-97.4	27.1	6.2	-2.2	7.3	**186.4**	18.7	-20.1	-9.5
	Lower		2020s	-20.5	-7.2	8.1	8.6	15.4	14.2	-5.8	-7.1	19.6	4.7	-11.7	4.3
			2050s	11.0	-10.2	6.5	-15.1	36.8	7.0	2.0	-11.4	30.0	9.1	-20.4	67.6
		1db19	2080s	36.2	-14.0	3.7	-31.3	44.1	-14.1	-14.7	-0.1	71.8	7.2	-37.2	61.2
			2020s	-22.6	-4.4	-28.6	-8.8	25.0	20.3	8.6	-1.0	-1.4	-16.9	-8.7	102.7
			2050s	16.1	-18.0	-10.6	-51.3	7.5	15.1	7.0	-11.7	-16.7	-15.4	-24.4	34.9
		1db17	2080s	47.0	-35.3	-18.0	-53.7	20.0	-6.9	5.4	-6.8	-9.7	-10.7	-38.3	64.7
LUENGERA	Upper		2020s	-12.5	-3.4	8.0	8.5	17.1	-2.6	14.0	5.1	21.8	11.2	1.3	-17.6
			2050s	-23.2	-6.5	12.1	-14.9	41.0	-39.3	12.1	4.5	33.4	-6.9	35.4	-67.4
		1da3	2080s	-24.8	-10.8	26.2	-30.8	49.0	-36.2	6.5	6.6	79.7	-12.1	6.3	-27.7
	Lower		2020s	-20.7	-5.4	-4.2	-21.3	29.0	-2.2	3.0	-3.5	15.3	2.9	-47.8	-29.1
			2050s	-29.0	-24.5	-11.5	-79.7	2.0	-9.1	4.9	-3.0	23.4	9.8	-27.3	-84.3
		1da1	2080s	-41.1	-17.2	-12.3	-83.0	12.1	-24.2	14.6	-2.2	55.8	5.1	6.1	-93.6
ESTUARY			2020s	-10.4	-3.4	-3.8	-30.4	11.7	-6.1	-10.0	4.0	10.6	18.1	-14.6	-26.3
			2050s	-11.3	-33.5	-14.6	101.5	11.6	-12.3	-7.3	20.5	-23.7	6.4	-22.6	-77.7
		Estuary	2080s	-12.6	-47.5	-11.0	-31.4	8.9	-60.0	-18.8	49.1	-26.2	-4.2	-47.9	-64.7

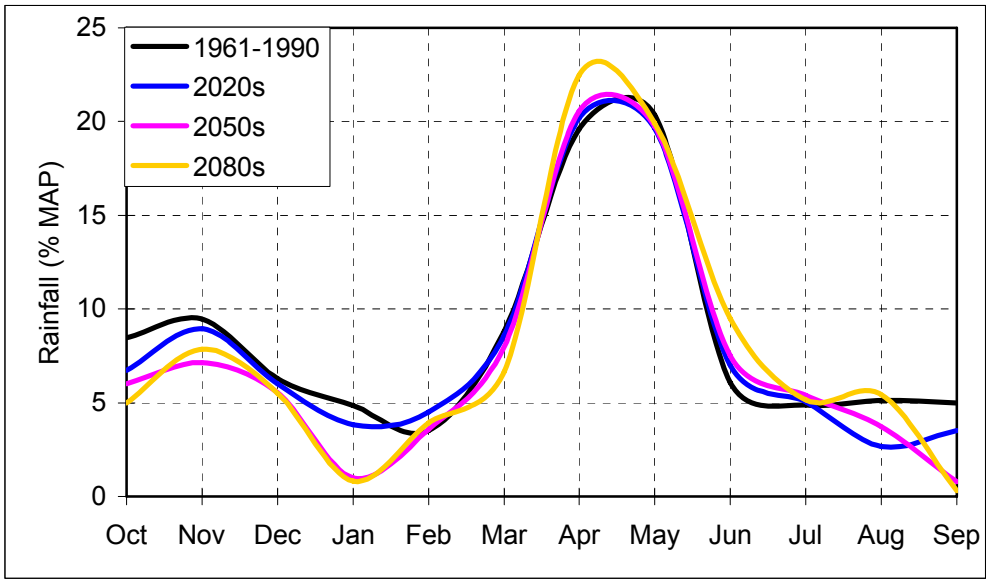

(a)

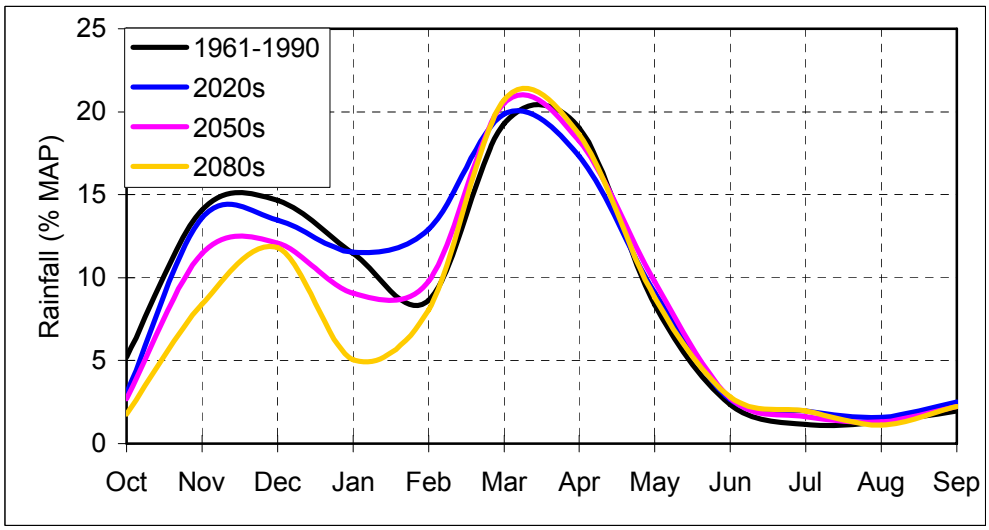

(b)

Fig 4.3: Rainfall changes between 1961 and 2099 at a) 1da1 and b) 1d10.

4.3.1.3 Discussion of developed future rainfall scenarios

The predicted changes of annual rainfall in Pangani indicate a general and predominant decline with some pockets of increasing annual rainfall in the Usambara Mountains (1d17, 1db19, 1db18, 1da3) along the Indian Ocean coast despite an increase in the immediate future (Table 4.8). Although these changes could be contradicting the general global picture of increasing rainfall over East Africa by the end of the 21st Century relative to the 1980-1999 reference period (IPCC 2007), the close analysis of predictions of annual rainfall in northeast Tanzania (Fig S11.13 in IPCC 2007) indicates that 11 out of the 21 GCMs predicted a decrease in or closest to the region. They include CGCM3.1 T63, PCM, CSIRO Mk 3.1, GFDL2.1, GISS – EH, GISS – ER, HadCM3, HadGEM1, IPSL – CM4, MIROC3.2 hires and ECHAM5/MPI – OM.

Table 4.8: Predicted changes (%) of seasonal rainfall in Pangani expressed from the 1980-1999 averages. Decreases are yellow filled, increases are light blue filled.

Sub-basin		Station	Period	SON	DJF	MAM	JJA	Annual
Kikuletwa	Upper	1dd55	2020s	-0.6	29.6	-1.7	24.0	7.8
			2050s	-15.1	21.2	-7.3	17.2	-0.2
			2080s	-38.2	9.3	-5.4	12.3	-6.4
	Lower	1dd54	2020s	3.5	12.2	-0.2	10.5	4.1
			2050s	-23.2	-18.0	-1.8	10.0	-8.9
			2080s	-51.5	-17.3	-1.7	-14.5	-14.1
		1dd1	2020s	11.4	16.6	-1.5	10.0	4.4
			2050s	-9.0	-8.1	-0.2	7.5	-2.1
			2080s	-46.5	-13.9	7.7	-1.2	-4.0
RUVU	Upper	1dc11	2020s	-26.6	4.6	4.1	21.4	0.0
			2050s	-44.9	-51.2	15.5	33.8	-8.1
			2080s	-79.7	-53.1	19.6	24.9	-14.2
	Lower	1dc2a	2020s	-4.5	10.1	9.0	30.4	7.8
			2050s	-8.9	-48.2	13.2	32.5	-5.4
			2080s	-14.1	-37.9	13.1	20.3	-4.9
		1dc1	2020s	-4.6	-3.4	4.4	-0.7	1.2
			2050s	-14.5	-43.0	-0.3	-4.4	-10.2
			2080s	-29.6	-43.3	4.8	-12.0	-10.1
PANGANI MAIN	Upper	1d10	2020s	-8.8	9.9	-0.6	64.8	3.5
			2050s	-21.7	-10.3	4.2	51.3	-4.0
			2080s	-40.8	-27.8	3.3	58.3	-13.6
	Middle	1d14	2020s	14.4	9.8	-7.1	11.6	2.1
			2050s	4.9	0.7	-8.9	14.6	-1.8
			2080s	8.0	-14.1	-6.2	0.0	-4.2
	Lower	1d17	2020s	21.3	9.0	-4.5	7.5	4.2
			2050s	11.6	-4.9	-0.6	7.4	2.4
			2080s	9.0	-3.0	9.0	-7.2	5.1
MKOMAZI	Upper	1db2a/1db18	2020s	-2.4	-7.7	14.7	62.5	4.7
			2050s	-36.3	11.6	13.8	63.5	4.2
			2080s	-62.1	-32.0	9.8	80.5	-18.1
	Lower	1db19	2020s	-3.7	6.9	3.1	9.3	3.5
			2050s	10.4	4.1	2.7	13.9	5.4
			2080s	14.7	-0.4	-6.9	30.4	1.9
		1db17	2020s	11.7	-7.9	11.4	-11.5	4.1
			2050s	6.6	-18.4	5.8	-21.6	-3.2
			2080s	7.3	-19.2	0.1	-20.1	-5.7
LUENGERA	Upper	1da3	2020s	5.1	9.3	9.5	22.1	10.4
			2050s	-10.3	9.2	0.1	31.4	4.6
			2080s	-5.8	11.7	-0.5	43.3	7.2
	Lower	1da1	2020s	1.0	10.1	-4.8	-4.7	-1.7
			2050s	-26.6	-22.4	-5.0	7.5	-9.5
			2080s	-30.8	-21.3	-3.6	29.8	-5.9
ESTUARY		Estuary	2020s	-3.5	-10.8	-9.4	1.3	-6.6
			2050s	-29.5	24.3	-3.8	-16.7	-7.9
			2080s	-33.7	-15.1	-7.7	-28.8	-18.2

The changes at the annual timescale could be derived from changes at the seasonal timescale. Except for a SON rainfall increase in the Usambaras, there is a general decline of SON rainfall in the Pangani basin while decreasing January rainfall is outweighed by increasing February and December rainfall to result in DJF rainfall increase in the immediate future although the decline is predicted towards the middle and the end of the 21st Century (Table 4.8). The increase total

rainfall in DJF is consistent with MM5 RCM predictions for the eastern part of Southern Africa (Tadross *et al*. 2005 as in IPCC 2007).

The general increase of the long (MAM) rains is predicted in areas stretching from Mount Kilimanjaro (Ruvu) southwards to the Usambara (Mkomazi) by the middle of the 21st Century and slight declining is predicted in the Usambaras by the end of the century. The predicted increase of MAM rainfall from downscaled scenarios is consistent with GCM predictions (URT VPO, 2003; OECD, 2003).

Predictions for the dry season are interesting as they depict a pattern that somehow contradicts results of previous studies. Despite known predictions of decreasing dry season (June-September, JJAS) rainfall in northeast Tanzania (URT VPO, 2003; OECD, 2003, IPCC, 2007b), results from the application of developed MLR models indicate an increase of JJAS seasonal rainfall (Table 4.8) attributed by the predominant increase of June and July rainfall and a general rainfall decline in August (Table 4.7). However, the percentage increase is declining towards the end of the 21st Century. The results are consistent with the predicted increase of JJAS from downscaled scenarios using six different GCM outputs (Fig 11.3 in IPCC 2007; Hewitson and Crane, 2006).

4.3.1.4 Rainfall series for wet and dry conditions

To account for possibility of future wetter or drier conditions in the basin, it was assumed that the post-1980s variance inherent in the observed series will prevail in the future. This might not be the case but is concurrent with the modelling process and assumptions. Analysis of observed rainfall series indicated that monthly values above 2 ($\mu + 2\sigma$) or below 1.5 (($\mu - 1.5\sigma$) standard deviations from the long-term averages (μ)are experienced in very few extremely wet (dry) years (e.g. Fig 4.4). According to criteria we developed for classification of wetness and dryness of the year using monthly and seasonal rainfall (see e.g. Juma, 2006; Tumbo, 2007), the frequently recurring events are the wet and dry events typically indicated by anomalies between 0.5 and 1.5 (average 1.0) and -0.5 and -1.5 (average -1.0) respectively. Therefore, to account for future possible wetter conditions, the average conditions series are modified by multiplication of a factor $(\mu + 1\sigma)/\mu$. Similarly, time series for drier conditions are computed by multiplying the average condition series by the factor $(\mu - 1\sigma)/\mu$. The 2050 average condition series for November at 1DC2A, for example, is multiplied by 1.434 and 0.566 to obtain series for anticipated wet and dry conditions respectively (Fig 4.5). This procedure established new monthly rainfall series for wetter and drier conditions, which are provided as separate MS Excel worksheet as part of this document.

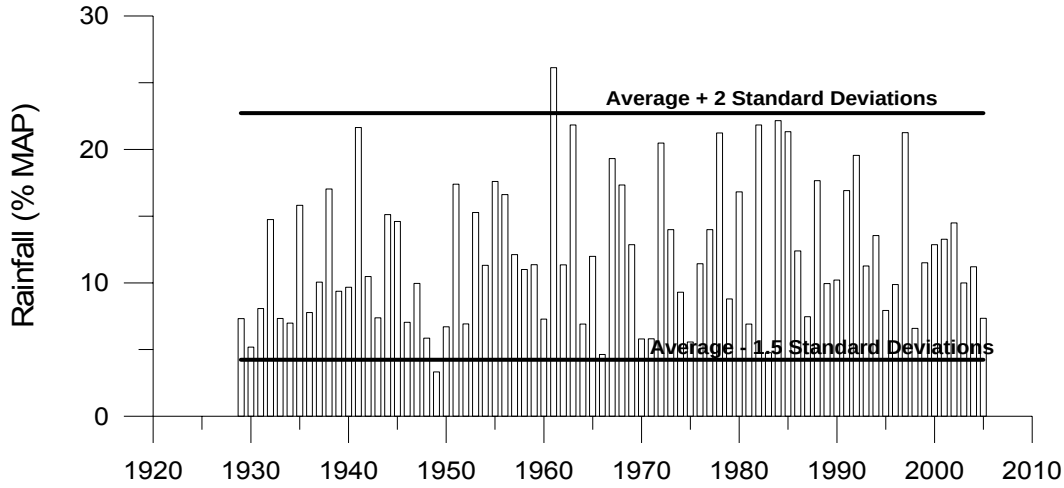

Fig 4.4: Time series of observed November catchment rainfall at 1DC2A.

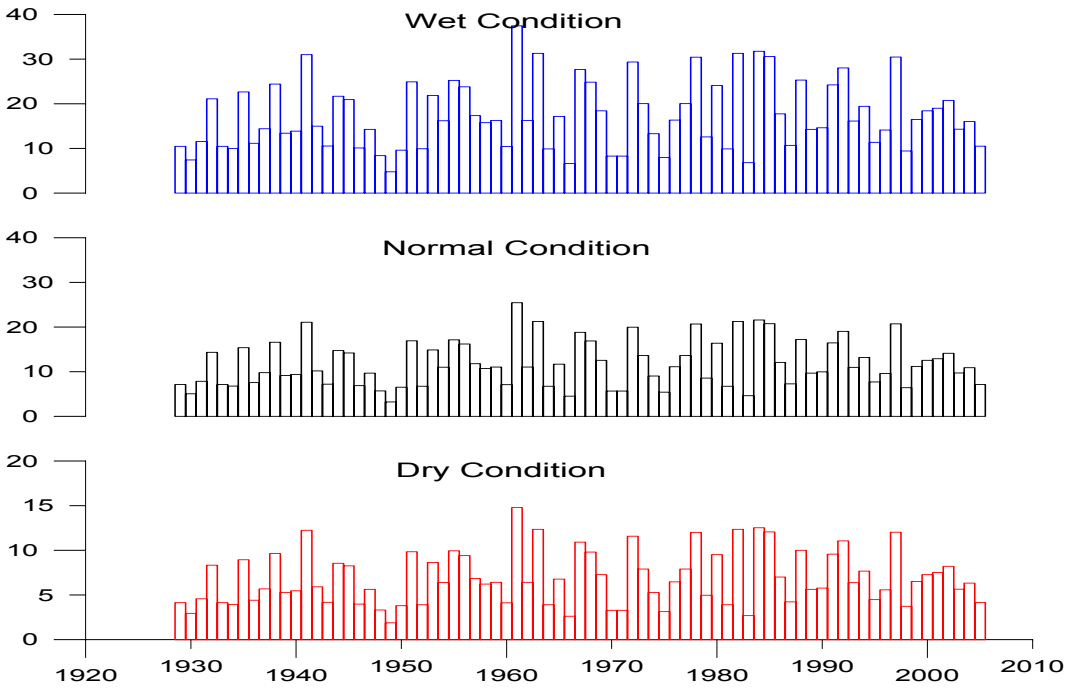

Fig 4.5: Time series of 2050 November rainfall amounts at 1DC2A for average, wetter and drier conditions.

4.3.2 Modified evaporation series

Owing to unavailability of time series of evaporation for the 16 selected catchments, the empirical method was proposed to provide modification of the available average monthly evaporation (Table 4.9). Since the evaporation change at the annual timescale is more accurately estimated by models than changes at monthly or seasonal timescales, annual evaporation were calculated from monthly evaporation for each catchment. The future changes to annual evaporation were then distributed across the 12 months with some modifications to account for predicted non-uniform temperature increases within the year.

Table 4.9: Available average monthly evaporation (mm) in Pangani basin.

Catchment	Oct	Nov	Dec	Jan	Feb	Mar	Apr	May	Jun	Jul	Aug	Sep	Annual
1dd55	186	193	177	208	184	208	163	146	124	128	146	163	2027
1dd54	204	191	190	199	202	204	167	142	135	135	155	180	2104
U/s NyM	195	180	177	186	180	182	154	124	120	120	142	163	1922
Dc10	204	210	217	221	186	213	171	135	133	133	153	174	2149
1db2a/1db17	164	171	173	182	176	177	150	128	116	120	128	146	1831
Db19 and da3	137	137	142	173	156	146	116	102	90	97	111	124	1531
D14	208	206	206	208	188	202	171	146	139	137	159	182	2153
Da1 d17a inc	133	141	155	173	168	168	124	111	107	106	106	116	1609
D17 and estuary	155	150	164	174	165	167	138	124	117	115	124	138	1731

Although present-day evaporation data is available at the monthly timescale, the available GCM projections of evaporation for Pangani are available at the annual timescale. IPCC (2001) indicate that future evaporation in Tanzanian basins may increase by between 10 – 25% by the year 2100. Therefore, this annual evaporation needs be redistributed in individual 12 months of the year and the following procedure was used:

i) Estimation of annual evaporation as sum of monthly evaporation
ii) Computation of monthly contributions to annual evaporation as ratios of monthly evaporation to annual evaporation
iii) Establishing modification factors for future monthly evaporation as equal to the delta change at the annual timescale for each future period (2020s, 2050s, 2080s)
iv) Adjustment of modification factors according to the effects of differential evaporation increase between the 12 months due to differential temperature increases
v) Computation of delta change of average monthly evaporation as the product between the adjusted modification factors during the future period considered and present-day monthly evaporation
vi) Estimation of modified average monthly evaporation as the sum of present-day average monthly evaporation and delta changes of monthly evaporation for each future period

As the first step, average monthly evaporation rates were cumulated to produce annual evaporation (Table 4.9). According to GCMs estimates of evaporation for Pangani (OECD, 2003), an increase of 20% of annual evaporation was considered to occur in Pangani by 2100. Assuming a linear rate of 20%/93 years = 0.215%/year of evaporation increase across the 93 years between 2007 and 2100, incremental increases of 3.9%, 10.3% and 14.6% will occur by 2020s, 2050s and 2080s respectively. These predicted evaporation changes at the annual timescale are equally applied to average monthly evaporation. That is, average January evaporation, for example, is increased by 4%, 10% and 15% to provide estimates for the 2020s, 2050s and 2080s respectively. This is repeated for all months.

To account for differential projected temperature increases with higher increases during the austral winter months (June-August) than during austral summer (December-February), the adjustments were made to monthly contributions to annual evaporation based on projected temperature increases. According to OECD (2003), temperature in Pangani might increase by 1.0^{o}C, 1.5^{o}C and 2.6^{o}C in June-August and lower increase of 0.8^{o}C, 1.1^{o}C and 1.9^{o}C in December-

February by 2020s, 2050s and 2080s respectively. Hudson and Jones (2002) indicated an increase of 2-3°C (December-February) and 2.5-3.5°C (June-August) by 2080s in Pangani. The difference between the projected increases in austral winter and summer was usually around 1°C.

These non-uniform temperature increases suggest that under future climate, evaporation during austral winter months of June-August will have a higher contribution to annual evaporation while austral summer months of December-February will have a slightly reduced contribution. Therefore, an adjustment of monthly contribution is introduced to rescale contributions of monthly evaporation to account for such changes. This adjustment factor (AF) is computed as the ratio between temperature increases in winter and summer and ranges between 3.0/2.5 = 1.200 (from Hudson and Jones projections) and 2.6/1.9 = 1.368 (from OECD projections). Finally, a higher adjustment factor (1.368) was adopted as the final adjustment factor to introduce a higher change of contribution of evaporation during the JJA period. This is considered as more water is available for evaporation during this JJA period, which follows the main rainy season, the long rains than in the DJF. A similar increase in temperature in DJF and JJA is therefore likely to result in more evaporation increase during the JJA period than DJF.

Accordingly, monthly evaporation contributions in December-March were rescaled through division by the adjustment factors to rescale down while those in June-September were multiplied by the factors to rescale up. Therefore, for a 10% change of annual evaporation, the adjusted contribution for January evaporation, for example, was calculated as $\left(\frac{(10/100)}{1.368}\right) = 0.075$ while that for July is $\left\{\left(\frac{10}{100}\right)\times 1.368\right\} = 0.141$. The adjustment was not applied to contributions of April, May, October and November evaporation rates. The adjustment was carried out for all the three future periods representing the 2020s, 2050s and 2080s. Adjusted monthly contributions were used to calculate monthly evaporation modification factors as the 1 + AF (Tables 4.10 – 4.12). The modification factors were then multiplied by present-day average monthly evaporation to provide future modified evaporation series for the 2020s, 2050s and 2080s. The modified average monthly evaporation data are included as worksheet files.

Table 4.10: Adjusted modification factors for monthly evaporation in Pangani basin for the 2020s.

Catchment	Oct	Nov	Dec	Jan	Feb	Mar	Apr	May	Jun	Jul	Aug	Sep
1dd55	1.039	1.039	1.029	1.029	1.029	1.029	1.039	1.039	1.053	1.053	1.053	1.053
1dd54	1.039	1.039	1.029	1.029	1.029	1.029	1.039	1.039	1.053	1.053	1.053	1.053
U/s NyM	1.039	1.039	1.029	1.029	1.029	1.029	1.039	1.039	1.053	1.053	1.053	1.053
1dc10	1.039	1.039	1.029	1.029	1.029	1.029	1.039	1.039	1.053	1.053	1.053	1.053
1db2a/1db17	1.039	1.039	1.029	1.029	1.029	1.029	1.039	1.039	1.053	1.053	1.053	1.053
1db19 and da3	1.039	1.039	1.029	1.029	1.029	1.029	1.039	1.039	1.053	1.053	1.053	1.053
1d14	1.039	1.039	1.029	1.029	1.029	1.029	1.039	1.039	1.053	1.053	1.053	1.053
1da1/ d17a inc	1.039	1.039	1.029	1.029	1.029	1.029	1.039	1.039	1.053	1.053	1.053	1.053
1d17 and estuary	1.039	1.039	1.029	1.029	1.029	1.029	1.039	1.039	1.053	1.053	1.053	1.053

Table 4.11: Modification factors for monthly evaporation in Pangani basin for the 2050s.

Catchment	Oct	Nov	Dec	Jan	Feb	Mar	Apr	May	Jun	Jul	Aug	Sep
1dd55	1.103	1.103	1.075	1.075	1.075	1.075	1.103	1.103	1.141	1.141	1.141	1.141
1dd54	1.103	1.103	1.075	1.075	1.075	1.075	1.103	1.103	1.141	1.141	1.141	1.141
U/s NyM	1.103	1.103	1.075	1.075	1.075	1.075	1.103	1.103	1.141	1.141	1.141	1.141
1dc10	1.103	1.103	1.075	1.075	1.075	1.075	1.103	1.103	1.141	1.141	1.141	1.141
1db2a/1db17	1.103	1.103	1.075	1.075	1.075	1.075	1.103	1.103	1.141	1.141	1.141	1.141
1b19 and 1da3	1.103	1.103	1.075	1.075	1.075	1.075	1.103	1.103	1.141	1.141	1.141	1.141
1d14	1.103	1.103	1.075	1.075	1.075	1.075	1.103	1.103	1.141	1.141	1.141	1.141
1da1/ d17a inc	1.103	1.103	1.075	1.075	1.075	1.075	1.103	1.103	1.141	1.141	1.141	1.141
1d17 and estuary	1.103	1.103	1.075	1.075	1.075	1.075	1.103	1.103	1.141	1.141	1.141	1.141

Table 4.12: Modification factors for monthly evaporation in Pangani basin for the 2080s.

Catchment	Oct	Nov	Dec	Jan	Feb	Mar	Apr	May	Jun	Jul	Aug	Sep
1dd55	1.146	1.146	1.107	1.107	1.107	1.107	1.146	1.146	1.200	1.200	1.200	1.200
1dd54	1.146	1.146	1.107	1.107	1.107	1.107	1.146	1.146	1.200	1.200	1.200	1.200
U/s NyM	1.146	1.146	1.107	1.107	1.107	1.107	1.146	1.146	1.200	1.200	1.200	1.200
1dc10	1.146	1.146	1.107	1.107	1.107	1.107	1.146	1.146	1.200	1.200	1.200	1.200
1db2a/1db17	1.146	1.146	1.107	1.107	1.107	1.107	1.146	1.146	1.200	1.200	1.200	1.200
1db19 and 1da3	1.146	1.146	1.107	1.107	1.107	1.107	1.146	1.146	1.200	1.200	1.200	1.200
1d14	1.146	1.146	1.107	1.107	1.107	1.107	1.146	1.146	1.200	1.200	1.200	1.200
1da1/ d17a inc	1.146	1.146	1.107	1.107	1.107	1.107	1.146	1.146	1.200	1.200	1.200	1.200
1d17 and estuary	1.146	1.146	1.107	1.107	1.107	1.107	1.146	1.146	1.200	1.200	1.200	1.200

The resulting projected monthly contributions still conserve the pattern of seasonal variation with the highest evaporation during the peak of austral summer (DJF) and lowest during austral winter (JJA) (Table 4.13). The comparison of individual monthly contributions between the present and 2080s indicated slight increase of 0.3-0.4% of the contribution during the austral winter (JJA) and similar decrease of 0.3-0.4% of the contribution during the austral summer (DJF) by 2080s (Table 4.13). The increases during the JJA period have resulted into contributions of monthly evaporation comparable and sometimes exceeding that in May.

The changes at the annual scale correspond to a total increase of 222-316 mm across the Pangani basin (Table 4.14). At the monthly timescale, the results indicate that highest changes of average monthly evaporation will be experienced during the winter months particularly at its end in September (23-36 mm) while the lowest changes in May (15-21 mm) and December (15-23 mm). Overall, the total increase of evaporation during the period June-September (JJAS) will account for 38-39% of the total annual evaporation increase by 2080s while the increase during the short (OND) and long (MAM) rains will separately account for 24-27% and 21-23% respectively. The January-February (JF) transition period will account for between 13% and 16% of annual evaporation change.

Table 4.13: Present-day and 2080s projected changes (%) of monthly evaporation in Pangani: Highest – red, Lowest – blue.

PRESENT-DAY

SNo	Catchment	Oct	Nov	Dec	Jan	Feb	Mar	Apr	May	Jun	Jul	Aug	Sep
1	1dd55	9.2	9.5	8.7	10.3	9.1	10.3	8.0	7.2	6.1	6.3	7.2	8.0
2	1dd54	9.7	9.1	9.1	9.5	9.6	9.7	7.9	6.7	6.4	6.4	7.4	8.6
3	U/s NyM	10.1	9.4	9.2	9.7	9.4	9.4	8.0	6.5	6.2	6.2	7.4	8.5
4	1dc10	9.5	9.8	10.1	10.3	8.7	9.9	8.0	6.3	6.2	6.2	7.1	8.1
5	1db2a/1db17	9.0	9.4	9.4	9.9	9.6	9.7	8.2	7.0	6.3	6.5	7.0	8.0
6	1db19 and 1da3	9.0	9.0	9.3	11.3	10.2	9.5	7.6	6.7	5.9	6.4	7.2	8.1
7	1d14	9.7	9.6	9.6	9.7	8.7	9.4	8.0	6.8	6.5	6.4	7.4	8.5
8	1da1/1d17a inc	8.3	8.8	9.6	10.7	10.4	10.5	7.7	6.9	6.7	6.6	6.6	7.2
9	1d17 and estuary	9.0	8.7	9.5	10.0	9.5	9.7	8.0	7.2	6.8	6.6	7.2	8.0

2080S

SNo	Catchment	Oct	Nov	Dec	Jan	Feb	Mar	Apr	May	Jun	Jul	Aug	Sep
1	1dd55	9.2	9.5	8.4	9.9	8.8	9.9	8.0	7.2	6.4	6.6	7.5	8.4
2	1dd54	9.7	9.1	8.7	9.1	9.3	9.3	7.9	6.7	6.7	6.7	7.7	9.0
3	U/s NyM	10.1	9.4	8.9	9.3	9.0	9.1	8.0	6.4	6.5	6.5	7.7	8.9
4	1dc10	9.5	9.8	9.8	10.0	8.4	9.6	8.0	6.3	6.5	6.5	7.4	8.5
5	1db2a/1db17	9.0	9.4	9.1	9.6	9.3	9.3	8.2	7.0	6.6	6.8	7.3	8.3
6	1db19 and 1da3	9.0	9.0	8.9	10.9	9.8	9.2	7.6	6.7	6.2	6.7	7.6	8.5
7	1d14	9.7	9.5	9.2	9.3	8.4	9.0	8.0	6.8	6.8	6.7	7.7	8.9
8	1da1/1d17a inc	8.3	8.8	9.3	10.4	10.1	10.1	7.7	6.9	7.0	6.9	6.9	7.5
9	1d17 and estuary	9.0	8.7	9.2	9.7	9.2	9.3	8.0	7.2	7.1	6.9	7.5	8.3

Table 4.14: 2080s projected changes (mm) of monthly evaporation in Pangani.

SNo	Catchment	Oct	Nov	Dec	Jan	Feb	Mar	Apr	May	Jun	Jul	Aug	Sep	Annual
1	1dd55	27.2	28.2	18.9	22.2	19.6	22.2	23.8	21.3	24.8	25.7	29.2	32.5	295.6
2	1dd54	29.7	27.8	20.3	21.3	21.6	21.7	24.4	20.7	27.0	27.0	31.0	36.0	308.4
3	U/s NyM	28.4	26.3	18.9	19.8	19.2	19.4	22.5	18.1	24.0	23.9	28.3	32.5	281.4
4	1dc10	29.7	30.7	23.2	23.6	19.8	22.7	25.0	19.7	26.5	26.5	30.5	34.7	312.7
5	1db2a/1db17	23.9	25.0	18.4	19.4	18.8	18.9	21.9	18.8	23.1	23.9	25.7	29.1	266.9
6	1db19 and 1da3	20.0	20.0	15.1	18.4	16.6	15.6	16.9	14.9	18.0	19.5	22.1	24.8	222.0
7	1d14	30.4	30.0	22.0	22.2	20.1	21.5	25.0	21.3	27.8	27.4	31.9	36.4	316.0
8	1da1/1d17a inc	19.4	20.6	16.5	18.4	17.9	18.0	18.1	16.2	21.4	21.2	21.2	23.1	232.2
9	1d17 and estuary	22.6	21.9	17.5	18.5	17.6	17.9	20.1	18.1	23.4	22.9	24.8	27.6	253.0

5 CONCLUSIONS

The study has successful establish MLR models for the prediction of monthly rainfall in the selected 16 catchments in the Pangani River Basin. NCEP/NCAR reanalyses of zonal (u-) and meridional (v-) winds, geopotential heights, relative humidity (rhum) and mean sea level pressure (MSLP) were the main predictors calibrating the MLR models with observed monthly rainfall as predictands. Model efficiencies were predominantly moderate to better and the models could suitably be used for prediction of future monthly rainfall amounts in the catchments.

The selection of suitable GCMs, which was mainly based on i) the knowledge of regional and large-scale climatic variables that influence rainfall variations in Pangani and ii) the review of GCM capabilities to simulate dominant climatic features in the Indian Ocean, retained the HadCM3 and GFDL CM2.1 as the most suitable. The application of present-day outputs of HadCM3 resulted in poor simulation with frequent negative rainfall predictions. The use of GFDL CM2.1 outputs improved significantly rainfall prediction with no predictions of negative rainfalls. The resulting downscaled rainfall indicated significant changes would be experienced during the months October to January leading to the decline of predominantly orographic rainfall in these early austral summer months. An increase of rainfall is predicted during the long rains particularly in April and May and the dry season and February.

Literature information and available average monthly rainfall were used to provide future evaporation series for the selected 16 catchments in the Pangani basin. Linear trend analysis produced projections of annual evaporation change of 4%, 10% and 15% for the 2020s, 2050s and 2080s respectively from the 20% projected increase in the 2100. Adjustments of contributions of monthly evaporation to annual evaporation using projected seasonal temperature changes successfully redistributed projected annual evaporation changes across the 12 months. They indicated slight increase of 0.3-0.4% of the contribution during the austral winter (JJA) and similar decrease of 0.3-0.4% of the contribution during the austral summer (DJF) by 2080s. Consequently, it was found that these changes will results in a higher contribution of June-September (JJAS) evaporation change (38-39%) of the total change of annual evaporation by 2080s while the increase during the short (OND) and long (MAM) rains will separately account for 24-27% and 21-23% respectively of the increase in annual evaporation. The January-February (JF) transition period will account for between 13% and 16%.

6 REFERENCES

Beuster, J., Howard, G.J. and Lugomela, G.V (2006) Hydrology and System Analysis: Hydrology of the Pangani River basin, **Vol 1**, 197p.

Hudson, D.A. and Jones, R.G. (2002) Regional climate model simulations of present-day and future climates of Southern Africa, Hadley Centre Technical Note 39, 40p.

IPCC (1990) *Climate Change: The IPCC Scientific Assessment* (Eds. Houghton, J.T., Jenkins, G.J. & Ephraums, J.J.). Cambridge University Press, Cambridge. 365p.

IPCC (1992) *Climate Change 1992: The Supplementary Report to the IPCC Scientific Assessment* (Eds. Houghton, J.T., Callander, B.A. & Varney, S.K.). Cambridge University Press, Cambridge. 200p.

IPCC (2001) *Climate Change 2001: The Scientific Basis*. Contribution of Working Group I to the Third Assessment Report of the Intergovernmental Panel on Climate Change [Houghton, J.T., Ding, Y., Griggs, D.J., Noguer, M., van der Linden, P.J., Dai, X., Maskell, K. & Johnson, C.A. (eds.)]. Cambridge University Press, Cambridge, United Kingdom and New York, NY, USA, 881p.

IPCC (2007) *Climate Change 2007: The Physical Science Basis*. Contribution of Working Group I to the Fourth Assessment Report of the Intergovernmental Panel on Climate Change [Solomon, S., D. Qin, M. Manning, Z. Chen, M. Marquis, K.B. Averyt, M. Tignor and H.L. Miller (eds.)]. Cambridge University Press, Cambridge, United Kingdom and New York, NY, USA, 940p.

Juma, K. (2006) A Study of socio-economic and land use changes in the catchment of Lake Jipe, MSc Dissertation, University of Dar es Salaam.

Kerr, R. A. (1992) Unmasking a shifty climate system, *Science*, **255**, 1508 – 1510.

Leggett, J., Pepper, W.J. & Swart, R.J. (1992) Emissions scenarios for the IPCC: An Update. In: *Climate Change 1992: The Supplementary Report to the IPCC Scientific Assessment* (Eds. Houghton, J.T., Callander, B.A. & Varney, S.K.). Cambridge University Press, Cambridge, pp.69-95.

OECD (2003) Development and climate change in Tanzania: Focus on Mount Kilimanjaro, OECD, 72p.

Saji, N. H., Xie, S.-P. and Yamagata, T. (2006) Tropical Indian Ocean variability in the twentieth Century climate simulations, *J Climate*, **19**, 4397 – 4417.

Tumbo, M. (2007) Vulnerability and adaptation of wetland based livelihoods in relation to climate variability and extreme in Simiyu, Tanzania, MSc Dissertation, University of Dar es Salaam.

Trenberth, K. E. (1990) Recent observed interdecadal climate changes in the northern Hemisphere, *Bull. Amer. Meteorol. Soc*., **71**, 988 – 993.

Trenberth, K. E. and Hoar, T. J. (1996) The 1990-1995 El Niño-Southern Oscillation event: longest on record, *Geophys. Res. Lett.*, **23**, 57 – 60.

Trzaska, S., Moron, V. and Fontaine, B. (1996) Global atmospheric response to specific linear combination of the main SST modes. Part I: Numerical experiments and preliminary results, *Ann. Geophys*., **14**, 1066 – 1077.

URT VPO (2003) Initial National Communication of Tanzania, 166p.

Valimba, P. (2005) Rainfall variability in southern Africa, its influences on streamflow variations and its relationships with climatic variations, Unpublished PhD Thesis, Rhodes University.

Valimba, P. and Mkhandi, S. H. (2007) Predictability of the short rains in Northeast Tanzania, *In Mahé G (Sc Ed) Climatic and Anthropogenic Impacts on the Variability of Water Resources, UNESCO Technical Document in Hydrology, No. 80,* 11 – 18, UNESCO Paris.

Wang, B. (1995) Interdecadal changes in El Niño onset in the last four decades, *J. Climate*, **8**, 267 – 285.

APPENDICES

APPENDIX A SEASONALITY OF CLIMATIC INFLUENCES ON PANGANI RAINFALL

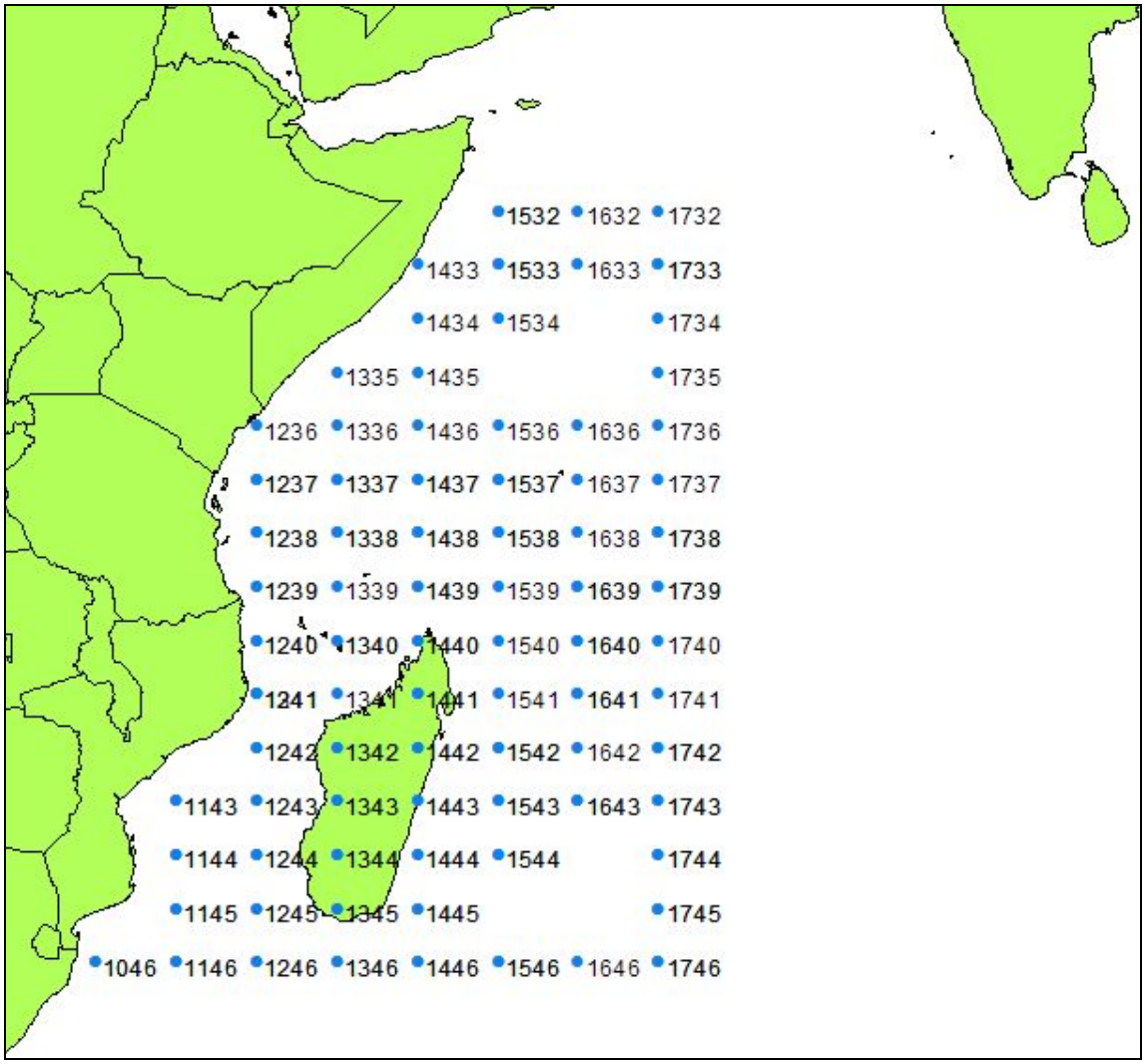

Fig A1: Gridbox identifiers

Table A.1: Seasonality of 850 hPa relative humidity predictors. The number is the gridbox identifier.

Jan	Feb	Mar	Apr	May	Jun	Jul	Aug	Sep	Oct	Nov	Dec
Grid											
1046	1239	1236	1143	1442	1236	1246	1144	1143	1237	1144	1143
1238	1341		1242	1444	1240	1536	1240	1145	1238	1145	1236
1240	1342		1243	1445	1243	1546	1243	1146	1239	1146	1238
1241	1345		1342		1341	1641	1340	1237	1240	1238	1336
1242	1346				1342	1646	1342	1242	1241	1239	1338
1244	1434				1542	1734	1346	1245	1246	1240	1344
1246	1437					1742	1440	1246	1335	1241	1436
1342	1439					1743	1441	1342	1435	1243	1532
1546	1536					1744	1442	1343	1442	1244	1533
1733	1537					1745	1443	1345	1532	1337	1534
1744	1636						1636	1346	1543	1341	1639
	1735						1646	1436	1546	1342	1640
	1736						1738	1438	1641	1343	1734
							1739	1442	1643	1435	1745
								1443	1646	1441	
								1444	1739	1543	
								1445	1742	1744	
								1446	1743		
								1534			
								1536			
								1537			
								1538			
								1544			
								1638			
								1738			
								1739			
								1744			
								1746			

Table A.2: Seasonality of surface zonal wind predictors. The number is the gridbox identifier.

Jan	Feb	Mar	Apr	May	Jun	Jul	Aug	Sep	Oct	Nov	Dec
Grid											
1237	1239	1242	1244	1339	1144	1143	1146	1046	1143	1240	1243
1239	1343	1244	1437	1342	1241	1238	1146	1146	1145	1340	1244
1240	1345	1337	1537	1442	1242	1239	1146	1240	1240	1342	1245
1241	1346	1340	1543	1443	1344	1243	1241	1346	1241	1343	1246
1244	1443	1342	1739	1541	1444	1339	1241	1438	1338	1343	1343
1246	1445	1437	1743	1546	1632	1343	1245	1443	1340	1344	1344
1340	1446	1441	1744	1641	1640	1346	1246	1444	1342	1344	1542
1341	1532	1537		1642	1733	1439	1433	1446	1346	1344	1543
1439	1533	1737		1746		1444	1440	1538	1433	1344	1738
1538	1538					1541	1445	1540	1437	1344	1742
1543	1539					1544	1445	1541	1442	1346	
1640	1544					1641	1445	1543	1446	1438	
1741	1744					1643	1737	1546	1537	1439	
						1741	1737	1633	1637	1444	
						1743	1737	1640	1641	1446	
								1641	1732	1533	
								1732	1740	1537	
								1733	1745	1539	
								1740		1546	
								1746		1637	
										1639	
										1641	
										1642	
										1740	
										1742	

APPENDIX B THE GFDL CM2.1 GCM

B1 INTRODUCTION

In 2004, a new family of GFDL climate models (the CM2.x family) was first used to conduct climate research. The GFDL CM2.x models have become the workhorse model for GFDL's climate research. They are being applied to topics focusing on decadal-to-centennial time scale issues (including multi-century control experiments and climate change projections), as well as to seasonal-to-interannual problems, such as El Niño research and experimental forecasts.

The CM2.x models share minimal genetic material with previous GFDL models. In other words, the CM2.x models belong to a completely different species than the older GFDL R30 and R15 coupled models. Accordingly, one should not expect results drawn from the newer CM2.x model experiments to be entirely consistent with those drawn from previous GFDL R30 and R15 experimental studies.

B2 MODEL STRUCTURE

The coupled model consists of four component models namely the atmosphere, land, sea-ice and ocean models. A coupler computes and passes fluxes between the component models and does all the necessary regridding so that each component receives inputs and supplies outputs on its own grid.

The atmospheric and land components

The atmosphere and land components resolution is 2° latitude × 2.5° longitude; the atmospheric model has 24 levels in the vertical. The model uses a 3-h time step for atmospheric radiation and a 0.5-h time step for other atmospheric physics and includes a diurnal cycle of insolation.

Atmospheric dynamics in GFDL CM2.1 are done using both a C and D grid. The dynamical core of the model uses FV numerics (Lin 2004). This difference alone accounts for changes in the surface wind stress pattern that lessen the drift after coupling. A tuning of the cloud scheme is introduced when using the FV core to achieve an approximate radiative balance while further tuning produced a small positive net radiative imbalance when using SSTs from the recent past.

The land model employed includes a river routing scheme that moves runoff collected over the model's drainage basins to river mouths, where the freshwater is injected into the model ocean. The land component model of CM2.1 is modified to suppress evaporation from land when soil is frozen at a depth of about 30 cm. This has a significant warming impact by reducing evaporation, and hence cloudiness, at higher latitudes of the northern hemisphere during late spring and summer, resulting in enhanced shortwave radiation at the surface and warmer near-surface air temperature.

The Ocean component

The ocean model formulation and physical parameterizations are based on the Modular Ocean Model code (MOM4; Griffies et al. 2003). The ocean model resolution is 1° in latitude and longitude, with meridional resolution equatorward of 30° becoming progressively finer, such that the meridional resolution is 1/3° at the equator. There are 50 vertical levels in the ocean, with 22 levels of 10-m thickness each in the top 220 m.

River flow into the ocean is predicted and is based upon a predetermined river drainage map determined from available global river networks and topographic maps. Any runoff from land cells is routed to an ocean discharge point, with a delay that varies from basin

to basin. The water is injected into the ocean evenly over the top 40 m (four levels) of the ocean.

The Sea-ice component

The sea ice component of is the GFDL Sea Ice Simulator (SIS). SIS is a dynamical model with three vertical layers, one snow and two ice, and five ice thickness categories. The elastic–viscous–plastic technique is used to calculate ice internal stresses, and the thermodynamics is a modified Semtner three-layer scheme.

The SIS model prognoses the velocity of the ice pack and the area and thermodynamic properties of ice and snow in five ice thickness categories. The snow layer has no heat capacity. The two ice layers are equally sized. Both have sensible heat capacity, and the upper layer, additionally, has latent heat capacity (brine). The brine content is calculated as a function of ice salinity and temperature as in the Bitz and Lipscomb (1999) model. The salinity of the ice for this purpose is set to mimic the behavior of the Semtner (1976) brine parameterization. A second ice salinity is used for calculating the salt flux between the ice and ocean that accompanies a given water flux. Ice is transferred between the three layers conservatively when there is snowfall, evaporation, melting, freezing or when the weight of the snow pushes it down below the waterline.

An upstream technique is used for advection of the five conservative quantities of ice concentration, snow mass, ice mass, ice upper layer enthalpy, and ice lower layer enthalpy. The thickness categories, which have no upper limits, are intended to resolve the thin end of the spectrum where ice grows rapidly and melts to form leads. The movement of ice between categories occurs by converting to conservative quantities, combining, and reconstituting conventional snow and ice properties from the conservative quantities.

Table B1: Sea ice model parameters.

Parameter	Value
Ice salinity (for brine content)	0.001
Ice salinity (for salt fluxes)	0.005
Snow albedo (dry/wet)	0.80/0.68
Ice albedo (dry/wet)	0.58/0.51
Ice strength parameters (P^*/c^*)	2.5×10^4 Pa/20
Ice/ocean drag coefficient (c_w)	3.24×10^{-3}
Ice surface roughness length	10^{-4} m
Ocean–ice thermal coupling	240 W m^{-2} K
Ice thickness category boundaries limits	0.1, 0.3, 0.7, 1.1 m

B3 MODEL EXPERIMENTS

The available experiments that are currently performed using GFDL CM2.1 are summarised in Table B1 and correspond to

i) **PICTNL:** the 1860 control; 500 years of output is available from these runs
ii) **1%to2X** & **1%to4X:** doubling and quadrupling of CO2, plus stabilization periods
iii) **20C3M (3 member ensembles):** the 1861-2000 'historical' runs; 140 years each
iv) **SRES A2:** 100 year long runs (2001-2100) following SRES A2 emission scenario

v) **SRES A1B** & **SRES B1:** 300 year long runs (2001-2300); stabilization post-2100

vi) **COMMIT:** 100 year long committed climate change experiments (2001-2100)

Table B1: GFDL CM2.1 experiments.

GFDL EXPERIMENT NAME	PCMDI EXPERIMENT NAME	EXPERIMENT DESCRIPTION
CM2.1U_Control-1860_D4	PIcntr (run1)	The pre-industrial control experiment
CM2.1U_Control-1990_E1	PDcntrl (run1)	The present-day control experiment
CM2.1U-D4_1860-2000-AllForc_H1	20C3M (run1)	The climate of the 20th Century experiment
CM2.1U-D4_1860-2000-AllForc_H2	20C3M (run2)	The climate of the 20th Century experiment
CM2.1U-D4_1860-2000-AllForc_H3	20C3M (run3)	The climate of the 20th Century experiment
CM2.1U-D4_1860-2000-AllForc_H4	20C3M (run4)	The climate of the 20th Century experiment
CM2.1U-D4_1860-2000-AllForc_H5	20C3M (run5)	The climate of the 20th Century experiment
CM2.1U-H2_Stable-2000_S1	Commit (run1)	The committed climate change experiment
CM2.1U-H2_SresA2_W1	SRESA2 (run1)	The SRES A2 experiment
CM2.1U-H2_SresA1B_X1	SRESA1B (run1)	The 720 ppm stabilization experiment (SRES A1B)
CM2.1U-H2_SresB1_Y1	SRESB1 (run1)	The 550 ppm stabilization experiment (SRES B1)
CM2.1U-H2_SresA1FI_Z1	SRESA1FI (run1)	Fossil fuel intensive experiment (SRES A1FI)
CM2.1U-D4_1PctTo2X_I1	1%to2x (run1)	A 1%/year CO2 increase experiment (to doubling)
CM2.1U-D4_1PctTo4X_J1	1%to4x (run1)	A 1%/year CO2 increase experiment (to quadrupling)

APPENDIX C THE HADCM3 GCM

C1 INTRODUCTION

HadCM3 is a coupled atmosphere-ocean GCM developed at the Hadley Centre and described by Gordon et al. (1999). It has a stable control climatology and does not use flux adjustment.

C2 MODEL STRUCTURE

The atmospheric component

The atmospheric component of the model has 19 levels with a horizontal resolution of 2.5 degrees of latitude by 3.75 degrees of longitude, which produces a global grid of 96 x 73 grid cells. This is equivalent to a surface resolution of about 417 km x 278 km at the Equator, reducing to 295 km x 278 km at 45 degrees of latitude.

A new radiation scheme is included with 6 and 8 spectral bands in the shortwave and longwave. The radiative effects of minor greenhouse gases as well as CO2, water vapour and ozone are explicitly represented. A simple parametrization of background aerosol is also included.

A new land surface scheme includes a representation of the freezing and melting of soil moisture, as well as surface runoff and soil drainage; the formulation of evaporation includes the dependence of stomatal resistance to temperature, vapour pressure and CO2 concentration. The surface albedo is a function of snow depth, vegetation type and also of temperature over snow and ice.

A penetrative convective scheme is used, modified to include an explicit down-draught, and the direct impact of convection on momentum. Parametrizations of orographic and gravity wave drag have been revised to model the effects of aniostropic orography, high drag states, flow blocking and trapped lee waves. The large-scale precipitation and cloud scheme is formulated in terms of an explicit cloud water variable following Smith. The effective radius of cloud droplets is a function of cloud water content and droplet number concentration.

The atmosphere component of the model also optionally allows the transport, oxidation and removal by physical deposition and rain out of anthropogenic sulphur emissions to be included interactively. This permits the direct and indirect forcing effects of sulphate aerosols to be modelled given scenarios for sulphur emissions and oxidants.

The Ocean component

The oceanic component of the model has 20 levels with a horizontal resolution of 1.25 x 1.25 degrees. At this resolution it is possible to represent important details in oceanic current structures.

Horizontal mixing of tracers uses a version of the adiabatic diffusion scheme with a variable thickness diffusion parametrization is used. There is no explicit horizontal diffusion of tracers. The along-isopycnal diffusivity of tracers is 1000 m^2/s and horizontal momentum viscosity varies with latitude between 3000 and 6000 m^2/s at the poles and equator respectively.

Near-surface vertical mixing is parametrized partly by a Kraus-Turner mixed layer scheme for tracers and a K-theory scheme for momentum. Below the upper layers the vertical diffusivity is an increasing function of depth only. Convective adjustment is modified in the region of the Denmark Straits and Iceland-Scotland ridge better to

represent down-slope mixing of the overflow water, which is allowed to find its proper level of neutral buoyancy rather than mixing vertically with surrounding water masses.

Mediterranean water is partially mixed with Atlantic water across the Strait of Gibraltar as a simple representation of water mass exchange since the channel is not resolved in the model.

The sea ice model uses a simple thermodynamic scheme including leads and snow-cover. Ice is advected by the surface ocean current, with convergence prevented when the depth exceeds 4 m.

There is no explicit representation of iceberg calving, so a prescribed water flux is returned to the ocean at a rate calibrated to balance the net snowfall accumulation on the ice sheets, geographically distributed within regions where icebergs are found. In order to avoid a global average salinity drift, surface water fluxes are converted to surface salinity fluxes using a constant reference salinity of 35 PSU.

The model is initialized directly from the Levitus (1994) observed ocean state at rest, with a suitable atmospheric and sea ice state. The atmosphere and ocean exchange information once per day. Heat and water fluxes are conserved exactly in the transfer between their different grids.